

A relaxed localized trust-region reduced basis approach for optimization of multiscale problems*

Tim Keil[†] and Mario Ohlberger[†]

March 21, 2022

In this contribution, we introduce and analyze a new relaxed and localized version of the trust-region method for PDE-constrained parameter optimization in the context of multiscale problems. As an underlying efficient discretization framework, we rely on the Petrov-Galerkin localized orthogonal decomposition method and its recently introduced two-scale reduced basis approximation. We derive efficient localizable a posteriori error estimates for the primal and dual equations of the optimality system, as well as for the two-scale reduced objective functional. While the relaxation of the outer trust-region optimization loop still allows for a rigorous convergence result, the resulting method converges much faster due to larger step sizes in the initial phase of the iterative algorithms. The resulting algorithm is parallelized in order to take advantage of the localization. Numerical experiments are given for a multiscale thermal block benchmark problem. The experiments demonstrate the efficiency of the approach, particularly for large scale problems, where methods based on traditional finite element approximation schemes are prohibitive or fail entirely.

Keywords: relaxed trust-region method, localized orthogonal decomposition, two-scale reduced basis approximation, multiscale optimization problems

AMS Mathematics Subject Classification: 49M20, 35J20, 65N15, 65N30, 90C06

1 Introduction

Parameterized multiscale problems where the parameters are optimized with respect to some user-defined quality criteria are of general interest in many physical, chemical, biomedical, or engineering applications. Examples, e.g., include optimal design of devices built from composed materials [8, 7, 19], optimization of reactive flow processes in porous media [37, 25, 58], or the design of meta-materials [17, 54, 50]. As a mathematical model for such constrained parameter optimization problems, we consider linear-quadratic parameter optimization, subject to the solution of a parameter-dependent elliptic variational multiscale problem.

The numerical approximation of such problems is computationally extremely demanding due to the multiscale character of the problem and the need for repeated PDE-solves within an outer iterative optimization loop. Recently, substantial progress has been made, both with respect to efficient algorithms for PDE-constrained optimization and with respect to efficient model order reduction approaches for variational multiscale problems.

***Funding:** The authors acknowledge funding by the Deutsche Forschungsgemeinschaft under Germany's Excellence Strategy EXC 2044 390685587, Mathematics Münster: Dynamics – Geometry – Structure and by the DFG under contract OH 98/11-1.

[†]Mathematics Münster, Westfälische Wilhelms-Universität Münster, Einsteinstr. 62, D-48149 Münster, tim.keil@uni-muenster.de, mario.ohlberger@uni-muenster.de

In the last two decades, there has been a tremendous development of suitable numerical methods for multiscale problems with the main intention to resolve the finest required scale only locally and collect the gathered fine-scale information in an effective coarse-scale global system. Well-established methods include the multiscale finite element method (MsFEM) [34, 22, 31], its generalized variants (GMsFEM) [23, 18], the heterogeneous multiscale method (HMM) [59, 21, 48], the variational multiscale method (VMM) [35, 36, 42], and the local orthogonal decomposition (LOD) [46, 30, 44].

For parameterized PDEs, model order reduction (MOR) has seen great development in the last decade [11]. A particular instance is the reduced basis method (RBM)[32, 57]. The main idea is a splitting into an offline- and online phase. In the offline phase, a sufficiently rich reduced basis (RB) is constructed with the full order model (FOM) that computes high-fidelity solutions. Subsequently, a projection-based surrogate model is build from the reduced basis. In the online phase, the resulting reduced order model (ROM) is evaluated with preferably no need to touch the high-fidelity complexity at all. In the context of parameter optimization for multiscale problems, model order reduction can be used to accelerate the repeated solving of the respective multiscale method.

Meanwhile, several applications of the RBM in the context of multiscale methods have been proposed in [23, 33, 47] for the MsFEM, in [1, 2, 3, 4, 5] for the HMM, in [6, 41] for the LOD and in [12, 51, 49, 53] for other related approaches. In the referenced works, the RBM has been used along with a parameterization of the local problems for speeding up the solution process of a single multiscale problem, whereas in [6, 47, 51, 49, 53, 41], a ROM is built for each individual local problem in the context of parameterized multiscale problems. For an overview of localized model order reduction and application to parameterized multiscale problems, we refer to the review article [14].

While the original idea of using the RBM within multiscale methods is to accelerate the solution procedures that are directly associated with the finest scale of the system, the resulting reduced methods are still computationally dependent on the coarse-mesh, and the global approximation error of the reduced system can often not be rigorously controlled. Recently in [41], these issues have been resolved by an additional reduction of the coarse system that is internally based on a two-scale formulation of the multiscale scheme.

In the context of PDE-constrained optimization, localized model order reduction with online enrichment has been suggested in [52]. The general idea of online enrichment algorithms is to specifically train the reduced models to the parameters that are queried during an optimization process. This idea has then been further investigated with rigorous analysis for global reduced basis approaches in the context of trust-region optimization methods [60, 56].

In this contribution, we will particularly build on a combination of the adaptive and certified trust-region reduced basis optimization method [39, 9, 40] with an underlying efficient discretization framework based on the Petrov-Galerkin LOD [24] and its recently introduced two-scale reduced basis approximation (TSRBLOD) [41]. The resulting variant of a trust-region localized RB method (TR-LRB) adaptively constructs local RB models in each of the TR subproblems and deviates from a classical globally resolved finite element approximation of the underlying multiscale state equation.

The application of error-aware TR methods with localized RB techniques is an original contribution of this article. As a necessary ingredient for an efficient adaptive reduced method, we will derive new localized error bounds for detecting where the model requires local basis updates and to find efficient global coupling techniques. As an explicit example, we use the localized RB technique for the LOD multiscale method (TSRBLOD) [41]. Following the ideas presented in [41], a posteriori error estimates are first derived for the primal and dual state equations of the optimality system. Based on these results, we finally obtain rigorous error bounds for the reduced objective functional, which is needed for the TR algorithm.

As a further original contribution, we introduce a relaxed version of the TR algorithm that allows for larger step sizes in the initial iterations of the TR-optimization loops without sacrificing the provable convergence of the overall method.

We emphasize that, as far as this contribution is concerned, using (localized) MOR to solve a single PDE-constrained parameter optimization problem aims to reduce the overall computational cost of the optimization method. Thus, neither offline- nor online computations of the LRB approach can be considered negligible.

Organization of the article The article is organized as follows: In Section 2, we detail the mathematical formulation of the considered multiscale optimization problem. In Section 3, we discuss the general formulation of a TR-LRB algorithm, including relaxation. Subsequently, in Section 4, we show that the TSRBLOD can be used as an instance of a TR-LRB algorithm. Lastly, in Section 5 we present numerical experiments that demonstrate the benefit of localized techniques.

2 Parameter optimization of multiscale problems

In this work, we are concerned with the efficient approximation of linear-quadratic parameter optimization, subject to a parameter-dependent multiscale variational state equation, which is typically given as a weak formulation of an underlying elliptic multiscale PDE.

To this end, let V denote a real-valued Hilbert space with inner product (\cdot, \cdot) and an induced norm $\|\cdot\|$, let $\mathcal{P} \subset \mathbb{R}^P$, with $P \in \mathbb{N}$ denote a compact and convex admissible parameter set, and $\mathcal{J}: V \times \mathcal{P} \rightarrow \mathbb{R}$ a linear-quadratic continuous functional with a parameter function $\Theta: \mathcal{P} \rightarrow \mathbb{R}$. Then, we seek for a local solution of the following PDE-constrained parameter optimization problem:

$$(P.a) \quad \min_{\mu \in \mathcal{P}} \mathcal{J}(u_\mu, \mu), \quad \text{with } \mathcal{J}(u, \mu) = \Theta(\mu) + j_\mu(u) + k_\mu(u, u),$$

subject to $u_\mu \in V$ being the solution of the *state – or primal – variational equation*

$$(P.b) \quad a_\mu(u_\mu, v) = l_\mu(v) \quad \text{for all } v \in V,$$

Moreover, we consider box-constraints of the form

$$\mathcal{P} := \{\mu \in \mathbb{R}^P \mid \mu_a \leq \mu \leq \mu_b\} \subset \mathbb{R}^P,$$

for given parameter bounds $\mu_a, \mu_b \in \mathbb{R}^P$, where “ \leq ” has to be understood component-wise. For each admissible parameter $\mu \in \mathcal{P}$, $a_\mu: V \times V \rightarrow \mathbb{R}$ denotes a continuous and coercive bilinear form, $l_\mu, j_\mu: V \rightarrow \mathbb{R}$ are continuous linear functionals and $k_\mu: V \times V \rightarrow \mathbb{R}$ denotes a continuous symmetric bilinear form. In this specific context, it is beneficial introduce the reduced cost functional $\hat{\mathcal{J}}: \mathcal{P} \rightarrow \mathbb{R}$, $\mu \mapsto \hat{\mathcal{J}}(\mu) := \mathcal{J}(u_\mu, \mu) = \mathcal{J}(S(\mu), \mu)$, where $S: \mathcal{P} \rightarrow V$ is the parameter to solution map of Equation (P.b). Then problem (P) is equivalent to the so-called reduced problem

$$(RP) \quad \min_{\mu \in \mathcal{P}} \hat{\mathcal{J}}(\mu).$$

We are particularly interested in multiscale applications in the sense that the parameter dependent bilinear form a_μ involves spatial heterogeneities. Throughout this contribution, we will consider the case for elliptic multiscale problems, where $V = H_0^1(\Omega)$, $\Omega \subset \mathbb{R}^d$, a_μ is given as

$$a_\mu(u_\mu, v) := \int_{\Omega} A_\mu(x) \nabla u_\mu(x), \nabla v(x) \, dx$$

and the family of diffusion or conductivity tensors $A_\mu: \Omega \rightarrow \mathbb{R}^{d \times d}$ have a rich multiscale structure that would lead to very high dimensional approximation spaces for the state space when approximated, e.g., with classical finite element type methods. As an example, we refer to Fig. 1 below for particular choices of such multiscale conductivity fields.

We employ standard assumptions on the underlying multiscale PDE. In particular, $A_\mu \in L^\infty(\Omega, \mathbb{R}^{d \times d})$ to be symmetric and uniformly elliptic, such that

$$(1) \quad 0 < \alpha := \text{ess inf}_{x \in \Omega} \inf_{v \in \mathbb{R}^d \setminus \{0\}} \frac{(A_\mu(x)v) \cdot v}{v \cdot v},$$

$$(2) \quad \infty > \beta := \text{ess sup}_{x \in \Omega} \sup_{v \in \mathbb{R}^d \setminus \{0\}} \frac{(A_\mu(x)v) \cdot v}{v \cdot v},$$

and we let $\kappa := \beta/\alpha$ be the maximum contrast of A_μ for all $\mu \in \mathcal{P}$. Moreover, let

$$l_\mu(v) := \int_{\Omega} f_\mu(x)v(x) \, dx$$

with $f_\mu \in L^2(\Omega)$. For $v \in V = H_0^1(\Omega)$, we define the standard (equivalent) norms:

$$\|v\|_1^2 := \int_{\Omega} |\nabla v(x)| \, dx, \quad \|v\|_{a,\mu}^2 := \int_{\Omega} |A_\mu^{1/2} \nabla v(x)| \, dx.$$

Note that $\|\cdot\|_1$ is a norm on V due to Friedrich's inequality, and $\|\cdot\|_{a,\mu}$ denotes the parameter-dependent energy norm. We emphasize that the homogeneous Dirichlet boundary conditions and the symmetry of A_μ are assumed for simplicity and to avoid technicalities in the definition and analysis of the TR-LRB method below. All the concepts elaborated in this paper can, however, be generalized to more complex cases of the underlying PDE.

As usual in the context of reduced basis methods, we require parameter separability for forms like a_μ , k_μ , l_μ , and j_μ as follows.

Assumption 1. *We assume a_μ , k_μ , l_μ , and j_μ to be parameter separable, i.e. there exist $\Xi_a, \Xi_l \in \mathbb{N}$ non-parametric components $a_q : V \times V \rightarrow \mathbb{R}$, $l_q : V \rightarrow \mathbb{R}$ for $1 \leq q \leq \Xi_a, \Xi_l$ and parameter functionals θ_q^a, θ_q^l , such that*

$$(3) \quad a_\mu(u, v) = \sum_{q=1}^{\Xi_a} \theta_q^a(\mu) a_q(u, v), \quad l_\mu(v) = \sum_{q=1}^{\Xi_l} \theta_q^l(\mu) l_q(v),$$

and analogously for k_μ and j_μ .

We note that the parameter separability of a_μ inherits from the separability of the coefficient matrix A_μ and is a standard assumption for RB methods. However, in lots of cases, this assumption needs to be artificially constructed with the help of the so-called Empirical Interpolation (EI) [10, 16, 20, 15]. For the sake of simplicity, we do not tackle this and let Assumption 1 always be fulfilled throughout this work.

Furthermore, to derive optimality conditions for (P), we require the following assumption:

Assumption 2 (Differentiability of a_μ , l_μ and \mathcal{J}). *We assume a_μ , l_μ , and \mathcal{J} to be Fréchet differentiable w.r.t each argument $u, v \in V$, and $\mu \in \mathcal{P}$. Given Assumption 1, this follows from assuming that also the separable parts of a_μ , l_μ , and \mathcal{J} are Fréchet differentiable.*

We define for given $u \in V$, $\mu \in \mathcal{P}$, the primal residual $r_\mu^{\text{pr}}(u) \in V'$ associated with (P.b) by

$$(4) \quad r_\mu^{\text{pr}}(u)[v] := l_\mu(v) - a_\mu(u, v) \quad \text{for all } v \in V.$$

In order to find a solution for Equation (P), we follow the approach of *first-optimize-then-discretize*, i.e. we deduce the first order necessary optimality system:

$$(5a) \quad r_{\bar{\mu}}^{\text{pr}}(\bar{u})[v] = 0 \quad \text{for all } v \in V,$$

$$(5b) \quad \partial_u \mathcal{J}(\bar{u}, \bar{\mu})[v] - a_\mu(v, \bar{p}) = 0 \quad \text{for all } v \in V,$$

$$(5c) \quad (\partial_\mu \mathcal{J}(\bar{u}, \bar{\mu}) + \nabla_\mu r_{\bar{\mu}}^{\text{pr}}(\bar{u})[\bar{p}]) \cdot (\nu - \bar{\mu}) \geq 0 \quad \text{for all } \nu \in \mathcal{P}.$$

From (5b), we observe the so-called *adjoint – or dual – equation*

$$(6) \quad a_\mu(q, p_\mu) = \partial_u \mathcal{J}(u_\mu, \mu)[q] = j_\mu(q) + 2k_\mu(q, u_\mu) \quad \text{for all } q \in V,$$

with solution $p_\mu \in V$ for a fixed $\mu \in \mathcal{P}$ and given the solution $u_\mu \in V$ to the state equation (P.b). For given $u, p \in V$, we introduce the dual residual $r_\mu^{\text{du}}(u, p) \in V'$ associated with (6) as

$$(7) \quad r_\mu^{\text{du}}(u, p)[q] := j_\mu(q) + 2k_\mu(q, u) - a_\mu(q, p) \quad \text{for all } q \in V.$$

We also note that sufficient conditions based on the Hessian can be used to verify that the stationary point is indeed a minimum. However, in our algorithms, this condition can always be checked posteriorly. For further details and references on the optimality system, we refer to [39].

3 Relaxation of the trust-region reduced basis method

We now introduce a relaxed variant of the error-aware adaptive TR-RB algorithm. The original algorithm is presented in [56, 60] and enhanced in [39, 9]. The proposed relaxation can be used as a warm start of the certified TR-RB algorithm but importantly fulfills the same convergence result asymptotically. The new variant – which we are going to define below – will be referred to as the relaxed TR-RB (R-TR-RB) method.

We start with a brief introduction of the basic TR-RB variant with full certification. To this end, let $\hat{\mathcal{J}}_h$ be a sufficiently accurate discrete version of $\hat{\mathcal{J}}$, meaning that the primal and dual equations above are discretized with an appropriate, probably high-dimensional, finite-dimensional space V_h . We denote this discrete reference model by the full order model (FOM), and make the following assumption.

Assumption 3 (The FOM is the “truth”). *We assume that the FOM discretization error $|\hat{\mathcal{J}}(\mu) - \hat{\mathcal{J}}_h(\mu)|$ can be neglected, meaning that $\hat{\mathcal{J}}_h$ defines an accurate full-order approximation. This also translates to the primal and dual approximation error being negligible.*

We note that we did not specify the concrete discretization scheme for computing $\hat{\mathcal{J}}_h$. In the original works [39, 56], this is based on a standard FEM approximation. However, as we see later, we choose multiscale methods as the underlying FOM method.

Moreover, we let $\hat{\mathcal{J}}_r$ denote a RB reduced functional of $\hat{\mathcal{J}}_h$ which is obtained by replacing the FOM with a reduced order model (ROM), where we will particular consider RB methods. We will assume that $\hat{\mathcal{J}}_r$ admits an a posteriori error result, such that

$$(8) \quad |\hat{\mathcal{J}}_h(\mu) - \hat{\mathcal{J}}_r(\mu)| \leq \Delta_{\hat{\mathcal{J}}_r}(\mu),$$

where $\Delta_{\hat{\mathcal{J}}_r}(\mu)$ can be computed without explicitly evaluating $\hat{\mathcal{J}}_h$ at $\mu \in \mathcal{P}$. We again emphasize that, in the original formulation, the reduced functional is based on a global RB method. We refer to [39, 9] for corresponding a posteriori error estimation results. If the reduced scheme instead stems from a localized model reduction approach, we abbreviate the resulting method as the TR-LRB method. A particular variant of such a localized approach will be discussed and analyzed below (see Proposition 4.7).

3.1 Trust-region reduced basis method

The TR-(L)RB algorithm iteratively computes a first-order critical (FOC) point of problem (P). In each outer iteration $k \geq 0$ of the TR, we utilize a model function $m^{(k)}$ as a local surrogate for the expensive objective functional \mathcal{J}_h . To construct the model function, we initialize the reduced model with the initial guess $\mu^{(0)} \in \mathcal{P}$.

As usual in TR methods, we then solve a sub-problem in the error-aware trust-region with radius $\delta^{(k)}$, characterized by the a posteriori error estimator of the surrogate. To this end, we choose

$$m^{(k)}(\cdot) := \hat{\mathcal{J}}_r^{(k)}(\mu^{(k)} + \cdot)$$

for $k \geq 0$, where the super-index (k) indicates that we use a progressively constructed RB space in each

iteration. We solve

$$(9) \quad \min_{\tilde{\mu} \in \mathcal{P}} \hat{\mathcal{J}}_r^{(k)}(\tilde{\mu}) \quad \text{s.t.} \quad \frac{\Delta_{\hat{\mathcal{J}}_r^{(k)}}(\tilde{\mu})}{\hat{\mathcal{J}}_r^{(k)}(\tilde{\mu})} \leq \delta^{(k)},$$

where $\tilde{\mu} := \mu^{(k)} + s$. As a solver for this sub-problem, we may choose the quasi-Newton projected BFGS algorithm combined with an Armijo-type condition and terminate with a standard reduced FOC termination criteria, modified with a projection on the parameter space $P_{\mathcal{P}}$ to account for constraints on the parameter space as proposed in [39]. It has been shown in [9] that a projected Newton algorithm for the sub-problems can enhance the convergence speed and accuracy. Additionally, we use a second boundary termination criterion for preventing the sub-problem from spending too much computational time on the boundary of the trust region. To be precise, at inner iteration l , we terminate the sub-problem optimization method if

$$(10a) \quad \|\mu^{(k,l)} - P_{\mathcal{P}}(\mu^{(k,l)} - \nabla_{\mu} \hat{\mathcal{J}}_r^{(k)}(\mu^{(k,l)}))\|_2 \leq \tau_{\text{sub}}$$

or

$$(10b) \quad \beta_2 \delta^{(k)} \leq \frac{\Delta_{\hat{\mathcal{J}}_r^{(k)}}(\mu^{(k,l)})}{\hat{\mathcal{J}}_r^{(k)}(\mu^{(k,l)})} \leq \delta^{(k)},$$

where $\tau_{\text{sub}} \in (0, 1)$ is a predefined tolerance and $\beta_2 \in (0, 1)$, generally close to one.

After the iterate $\mu^{(k+1)} := \mu^{(k,L)}$ has been computed after L inner optimization steps, the sufficient decrease conditions helps to decide whether to accept the iterate:

$$(11) \quad \hat{\mathcal{J}}_h(\mu^{(k+1)}) \leq \hat{\mathcal{J}}_r^{(k)}(\mu_{\text{AGC}}^{(k)}).$$

This condition can be cheaply checked by using a sufficient and necessary condition, cf. [39, 60]. However, if the cheap conditions are not applicable, we have to validate Equation (11) explicitly. If the iterate is rejected, we shrink the TR-radius and repeat the sub-problem. If instead, $\mu^{(k+1)}$ is accepted, we use the parameter to enrich the reduced model. Overall, convergence of the TR-RB algorithm can be verified with a FOM-based FOC condition

$$(12) \quad \|\mu^{(k+1)} - P_{\mathcal{P}}(\mu^{(k+1)} - \nabla_{\mu} \hat{\mathcal{J}}_h(\mu^{(k+1)}))\|_2 \leq \tau_{\text{FOC}},$$

where the FOM quantities are available from the enrichment. Moreover, these allow for computing a condition for possibly enlargement of the TR radius if the reduced model is better than expected, cf. [39]. Let us also mention that a reduced Hessian can be used to utilize an a posteriori post-processing result for the optimal parameter, cf. [9].

The convergence of the described TR-RB algorithm has been shown in [39] and has been further generalized in [9]. Moreover, the convergence is not affected by the choice of the reduction approach of the primal and dual equations, as long as a certified error control of the reduced functional is given. In the numerical experiments that were shown in [39, 9, 40], the TR-RB algorithm showed a remarkably robust behavior, including significant enhancements compared to the original version from [56]. Nevertheless, some hints for room for improvements concerning the overall cost were noticeable.

In what follows, we discuss problematic scenarios that may occur for the basic TR-RB algorithm as it is presented above. In many cases, the initial TR-radius $\delta^{(0)}$ chosen in the algorithm does not fit the underlying model and optimization problem. Thus, it is very likely to happen that, especially at the beginning of the TR-RB algorithm, the sufficient decrease condition (11) is not fulfilled after the sub-problem terminated according to (10). This eventually causes the algorithm to reject the parameter and shrink the TR-radius. The situation may repeat multiple times before a suitable TR-radius is found to ensure convergence of the algorithm.

If the TR-radius is shrunk, two scenarios in the algorithm can significantly harm the computational speed of the overall algorithm. First, if (11) can not be verified by the cheap conditions, we require

FOM evaluations at the current iterate. In the worst case, the iterate is rejected, and the TR-radius is shrunk, causing the FOM information to be ignored.

A second scenario is that the TR-radius of an accepted sub-problem occurs to be very small, no matter which of the above-described criteria causes repeated rejections of the iterate. As a matter of fact, the certified step by the TR-RB algorithm and also later outer iterations potentially do small steps towards the optimum because the cut-off from (10b) is tracked early. To tackle this, we introduced the possibility of enlarging the TR-radius in [39]. However, in an extreme scenario, the computational effort of the TR-RB algorithm may still significantly be harmed. Importantly, even if the TR-radius is not shrunk initially, the TR-radius can still prevent the algorithm from iterating as far as it potentially could (for instance, if the error estimator suffers severe overestimation). Furthermore, the choice of a "perfect" TR-radius and shrinking- or enlarging factors are problem-dependent and, at least to our knowledge, always have to be found by trials.

Another important slow-down factor of the TR-RB algorithm is the evaluation of the error estimator $\Delta_{\hat{\mathcal{J}}_r}$ or the construction of the offline-online decomposed version of it since it involves the computation of Riesz-representatives w.r.t. the inner product of V_h .

3.2 Relaxation of the method

Following the remarks above, we conclude that the full certification of the model can significantly slow down the convergence of the TR-RB algorithm, although potentially rejected iterates and model functions would still have been accurate enough to converge faster. With this in mind, in what follows, we introduce the relaxed TR-RB algorithm, where early certifications of the TR-RB algorithm are essentially ignored, and, instead, the TR methodology is only enforced in later iteration counts.

Let $(\varepsilon_{\text{TR}}^{(k)})_k$ and $(\varepsilon_{\text{cond}}^{(k)})_k$ be sequences of relaxation factors for the TR-radius and the sufficient decrease condition, respectively. Furthermore, we assume that both sequences are decreasing and strongly converge to zero, i.e.

$$(13) \quad \lim_{k \rightarrow \infty} \varepsilon_{\text{TR}}^{(k)} = 0 \quad \text{and} \quad \lim_{k \rightarrow \infty} \varepsilon_{\text{cond}}^{(k)} = 0.$$

After the surrogate model has been initialized with $\mu^{(0)}$, we solve the same problem as (9) but with relaxed trust-region. In detail, for every outer iteration k , we solve the relaxed TR sub-problem

$$(14) \quad \min_{\tilde{\mu} \in \mathcal{P}} \hat{\mathcal{J}}_r^{(k)}(\tilde{\mu}) \quad \text{s.t.} \quad \frac{\Delta_{\hat{\mathcal{J}}_r^{(k)}}(\tilde{\mu})}{\hat{\mathcal{J}}_r^{(k)}(\tilde{\mu})} \leq \delta^{(k)} + \varepsilon_{\text{TR}}^{(k)},$$

with the the same convergence criterion (10a) as before but with a relaxed version of the TR-related cut-off criterion (10b):

$$(15) \quad \beta_2(\delta^{(k)} + \varepsilon_{\text{TR}}^{(k)}) \leq \frac{\Delta_{\hat{\mathcal{J}}_r^{(k)}}(\mu^{(k,l)})}{\hat{\mathcal{J}}_r^{(k)}(\mu^{(k,l)})} \leq \delta^{(k)} + \varepsilon_{\text{TR}}^{(k)}.$$

After the sub-problem solver terminated, we accept the iterate with the relaxed version of (11), which reads

$$(16) \quad \hat{\mathcal{J}}_h^{(k+1)}(\mu^{(k+1)}) \leq \hat{\mathcal{J}}_r^{(k)}(\mu_{\text{AGC}}^{(k)}) + \varepsilon_{\text{cond}}^{(k)},$$

and can be quickly checked with the corresponding relaxed cheap surrogate criteria, cf. [39, 60]. Moreover, we evaluate the same FOM-based termination criterion Equation (12) as in the TR-RB algorithm. If the outer algorithm is not terminated, we enrich the model and again solve (14) until convergence. The rest of the algorithm can be followed analogously to the fully certified version.

Concerning the convergence, due to conditions (13) of the relaxation sequences, asymptotic convergence of the R-TR-RB algorithm can be proven along the same lines as in [9, Theorem 3.8], formulated in the following theorem:

Theorem 3.1 (Convergence of the R-TR-RB algorithm, cf. [9]). *Let $(\varepsilon_{TR}^{(k)})_k$ and $(\varepsilon_{cond}^{(k)})_k$ be relaxation sequences that fulfill (13) and let sufficient assumptions on the Armijo search to solve (14) be given; cf. [9]. Then every accumulation point $\bar{\mu}$ of the sequence $\{\mu^{(k)}\}_{k \in \mathbb{N}} \subset \mathcal{P}$ generated by the above described R-TR-RB algorithm is an approximate first-order critical point for $\hat{\mathcal{J}}_h$, i.e., it holds*

$$(17) \quad \|\bar{\mu} - \mathbf{P}_{\mathcal{P}}(\bar{\mu} - \nabla_{\mu} \hat{\mathcal{J}}_h(\bar{\mu}))\|_2 = 0.$$

Thus, the first iterations of the R-TR-RB algorithm can be considered a warm start for the algorithm that can already lead to early convergence. In practice, we can expect the identical numerical behavior of the two algorithms once $\varepsilon_{TR}^{(k)}$ and $\varepsilon_{cond}^{(k)}$ are below double machine-precision. As with all different optimization methods for the discussed optimization problems, it can always happen that the R-TR-RB algorithm finds a different local minimum than the originally proposed TR-RB algorithm.

The R-TR-RB algorithm can be considered a non-certified algorithm in the first iterations, meaning that $\varepsilon_{TR}^{(k)}$ and $\varepsilon_{cond}^{(k)}$ are chosen large enough, such that the error estimator can be ignored. In conclusion, for these cases, we do not have to prepare for the efficient computation of the error estimator, which further results in a significant speedup of the algorithm, cf. Section 5.

4 Optimization of multiscale problems based on the TSRBLOD

One of the main contributions of this article is to develop a TR-LRB method based on the TSRBLOD approach from [41], which is a reduction approach for the PG-LOD method [24]. All features of the (relaxed) TR-RB that we detailed in the previous section can naturally be used for the localized case simply by replacing the functional $\hat{\mathcal{J}}_h$ appropriately. Specific circumstances may occur depending on the localized reduction approach at hand, for instance, regarding the initial construction and enrichment of the localized surrogate.

In the following, we give a precise definition of a localized reduced FOM functional $\hat{\mathcal{J}}_h^{\text{loc}}$, the localized reduced ROM functional $\hat{\mathcal{J}}_r^{\text{loc}}$, and its gradient information $\nabla \hat{\mathcal{J}}_h^{\text{loc}}$, and $\nabla \hat{\mathcal{J}}_r^{\text{loc}}$, respectively. Furthermore, we elaborate on the error estimator $\Delta_{\hat{\mathcal{J}}_r^{\text{loc}}}$ and provide details on the localized online enrichment of the ROM.

4.1 Localized full order model using the LOD

The LOD is by now a well-established multiscale method that is particularly flexible for rough and non-periodic multiscale coefficients. Since we intend to use the PG-LOD as the FOM model of the optimality system (5), we now explain the primary concepts of the method. We refer to [44] for more background and to [41], where the same notation is used.

Localized orthogonal decomposition method Typical for multiscale methods, we use a low-dimensional coarse-mesh \mathcal{T}_H with mesh size $H \gg h$ and construct the respective FE space by $V_H := V_h \cap \mathcal{P}_1(\mathcal{T}_H)$. Subsequently, we define the corresponding ideal LOD space by

$$V_{H,\mu}^{\text{ms}} := (I - \mathcal{Q}_{\mu})(V_H).$$

Here, the fine-scale corrections $\mathcal{Q}_{\mu}(v) \in V_h^f$, for a given $v_h \in V_h$, are the solution of

$$(18) \quad a_{\mu}(\mathcal{Q}_{\mu}(v_h), v^f) = a_{\mu}(v_h, v^f) \quad \text{for all } v^f \in V_h^f,$$

where the fine-scale space $V_h^f := \ker(\mathcal{I}_H) \subset V_h$ can be obtained with a dedicated interpolation operator $\mathcal{I}_H : V_h \rightarrow V_H$ that maps a high-fidelity function $v_h \in V_h$ to the coarse FE space $v_H \in V_H$. In conclusion, $\mathcal{Q}_{\mu}(v_h)$ is the a_{μ} -orthogonal projection of v_h onto V_h^f , such that we have a_{μ} -orthogonal splitting of V_h , i.e., $V_h = V_{H,\mu}^{\text{ms}} \oplus_{a_{\mu}} V_h^f$.

Since both spaces are still defined on the whole computational domain, we use corresponding truncated fine-scale correctors $\mathcal{Q}_{\ell,\mu}^T(v) \in V_{h,\ell,T}^f$, where $V_{h,\ell,T}^f := V_h^f \cap H_0^1(U_{\ell}(T))$ is the localized fine-scale space

on patch $U_\ell(T)$ with size $\ell \in \mathbb{N}$ around each element T of the coarse FE-mesh. The resulting localized space can then be defined as

$$V_{H,\ell,\mu}^{\text{ms}} = (I - \mathcal{Q}_{\ell,\mu}^{\text{pr}})(V_H),$$

where $\mathcal{Q}_{\ell,\mu}$ contains localized corrector functions $\mathcal{Q}_{\ell,\mu}^T$, computed on the localized fine-scale spaces $V_{h,\ell,T}^f := V_h^f \cap H_0^1(U_\ell(T))$ and the localized variant of (18).

Finally, we approximate the solution of (P.b) by the Petrov–Galerkin version of the LOD: Find $u_{H,\ell,\mu}^{\text{ms}} \in V_{H,\ell,\mu}^{\text{ms}}$, such that

$$(19) \quad a_\mu(u_{H,\ell,\mu}^{\text{ms}}, v_H) = l_\mu(v_H) \quad \text{for all } v_H \in V_H.$$

We note that the standard Galerkin formulation can be obtained by using $V_{H,\ell,\mu}^{\text{ms}}$ also as the test function; see [44]. To ensure that (19) has a unique solution, we require inf-sup stability of a_μ w.r.t. $V_{H,\ell,\mu}^{\text{ms}}$ and V_H . As proposed in [41], an appropriate inf-sup stability constant is given by

$$\gamma_\ell^{\text{pg}} := \inf_{0 \neq w_H \in V_H} \sup_{0 \neq v_H \in V_H} \frac{a_\mu(w_H - \mathcal{Q}_{\ell,\mu}^T(w_H), v_H)}{\|w_H - \mathcal{Q}_{\ell,\mu}^T(w_H)\|_{a,\mu} \|v_H\|_1},$$

where the proof of the inf-sup stability is conditioned on sufficiently large ℓ and can be shown analogously to [24, 29].

Two-scale formulation In order to relate (19) to the two-scale-based view on the PG–LOD as used in [41], we further note that there exists a uniquely defined two-scale representation $\mathbf{u}_\mu \in \mathfrak{V}$ of $u_{H,\ell,\mu}^{\text{ms}} \in V_{H,\ell,\mu}^{\text{ms}}$, in the two-scale space

$$\mathfrak{V} := V_H \oplus V_{h,\ell,T_1}^f \oplus \cdots \oplus V_{h,\ell,T_{|\mathcal{T}_H|}}^f.$$

For $\mathbf{u} = (u_H, u_{T_1}^f, \dots, u_{T_{|\mathcal{T}_H|}}^f) \in \mathfrak{V}$ we define the corresponding two-scale H^1 -norm of \mathbf{u} by

$$\|\mathbf{u}\|_1^2 := \|u_H\|_1^2 + \sum_{T \in \mathcal{T}_H} \|u_T^f\|_1^2.$$

The two-scale approximation $\mathbf{u}_\mu \in \mathfrak{V}$ is the solution of

$$(20) \quad \mathfrak{B}_\mu(\mathbf{u}_\mu, \mathbf{v}) = \mathfrak{F}_\mu(\mathbf{v}) \quad \text{for all } \mathbf{v} \in \mathcal{V},$$

where we define the two-scale bilinear form $\mathfrak{B}_\mu \in \text{Bil}(\mathfrak{V})$ given by

$$\begin{aligned} \mathfrak{B}_\mu \left((u_H, u_{T_1}^f, \dots, u_{T_{|\mathcal{T}_H|}}^f), (v_H, v_{T_1}^f, \dots, v_{T_{|\mathcal{T}_H|}}^f) \right) := \\ a_\mu(u_H - \sum_{T \in \mathcal{T}_H} u_T^f, v_H) + \rho^{1/2} \sum_{T \in \mathcal{T}_H} a_\mu(u_T^f, v_T^f) - a_\mu^T(u_H, v_T^f), \end{aligned}$$

with a stabilization parameter $\rho \geq 1$; cf. [41]. Further, let $\mathfrak{F} \in \mathfrak{V}'$ be given as

$$\mathfrak{F}_\mu \left((v_H, v_{T_1}^f, \dots, v_{T_{|\mathcal{T}_H|}}^f) \right) := l_\mu(v_H).$$

As proven in [41], the two-scale solution $\mathbf{u}_\mu \in \mathfrak{V}$ can always be constructed from (19) and the respective fine-scale correctors, such that

$$(21) \quad \mathbf{u}_\mu = \left[u_{H,\ell,\mu}, \mathcal{Q}_{\ell,\mu}^{T_1}(u_{H,\ell,\mu}), \dots, \mathcal{Q}_{\ell,\mu}^{T_{|\mathcal{T}_H|}}(u_{H,\ell,\mu}) \right].$$

Approximation of the objective functional The corresponding primal state can now be used to compute the corresponding localized FOM objective functional, i.e.

$$(22) \quad \hat{\mathcal{J}}_h^{\text{loc}}(\mu) := \mathcal{J}(u_{H,\ell,\mu}, \mu).$$

Again, the subindex h in $\hat{\mathcal{J}}_h^{\text{loc}}$ refers to the fact that the construction of the solution space $V_{H,\ell,\mu}^{\text{ms}}$ for solving (19) internally requires the computation of the correctors that resolve the fine-scale mesh, which can then be discarded immediately. Note that we do not plugin $u_{H,\ell,\mu}^{\text{ms}} \in V_{H,\ell,\mu}^{\text{ms}}$ into \mathcal{J} since the basis of $V_{H,\ell,\mu}^{\text{ms}}$ may not be available. This is the case if the corrector problems can not be stored, which, in many cases, can be sufficient since the coarse-scale behavior is anyway captured by $u_{H,\ell,\mu} \in V_H$; cf. [24]. To align with this, we employ the following structural assumption on \mathcal{J} , which agrees with what is usually expected in a multiscale setting.

Assumption 4 (\mathcal{J} is a coarse functional). *We assume that the objective functional is a coarse functional, i.e. for all $u_H \in V_H$ and $u^f \in V_h^f$, we have*

$$\mathcal{J}(u_H + u^f, \mu) = \mathcal{J}(u_H, \mu).$$

To conclude, we are interested in solving the following reduced PDE-constrained parameter optimization problem

$$(\text{RPloc}) \quad \min_{\mu \in \mathcal{P}} \hat{\mathcal{J}}_h^{\text{loc}}(\mu).$$

Further approximation of the optimality system To solve (RPloc) with the TR-LRB algorithm, we require the gradient information of $\hat{\mathcal{J}}_h^{\text{loc}}$. In our approach, a dual model is utilized, which we also solve with the PG-LOD. While (19) works as a replacement for (P.b), we formulate a corresponding PG-LOD version of the dual problem for (6): Seek a function $p_{H,\ell,\mu}^{\text{ms}} \in V_{H,\ell,\mu}^{\text{ms}}$ such that

$$(23) \quad a_\mu(v_H, p_{H,\ell,\mu}^{\text{ms}}) = \partial_u \mathcal{J}(u_{H,\ell,\mu}, \mu)[v_H] \quad \text{for all } v_H \in V_H.$$

Note that Assumption 4 justifies that $u_{H,\ell,\mu}$ is used for the right-hand side of (23). Looking at (23), we conclude that, just as the FOM in [39], the localized FOM is a conforming choice in the sense that $u_{H,\ell,\mu}^{\text{ms}}$ and $p_{H,\ell,\mu}^{\text{ms}}$ belong to the same space $V_{H,\ell,\mu}^{\text{ms}}$. Note that this choice only makes sense if the given multiscale coefficient A_μ is symmetric, as we have assumed throughout this article. In that case, the recaptured multiscale effects for the primal and dual operator are the same. If instead A_μ is not symmetric, different LOD spaces must be constructed, which we do not consider.

With

$$(24) \quad \mathfrak{F}_{\mu, u_{H,\ell,\mu}}^{\text{du}} \left((v_H, v_{T_1}^f, \dots, v_{T_{|\mathcal{T}_H|}}^f) \right) := \partial_u \mathcal{J}(u_{H,\ell,\mu}, \mu)[v_H],$$

we can formulate the two-scale dual solution $\mathfrak{p}_\mu \in \mathfrak{V}$ of

$$(25) \quad \mathfrak{B}_\mu(\mathfrak{p}_\mu, \mathfrak{v}) = \mathfrak{F}_{\mu, u_{H,\ell,\mu}}^{\text{du}}(\mathfrak{v}) \quad \text{for all } \mathfrak{v} \in \mathcal{V},$$

where we note that we did not flip the arguments, due to the symmetry of a_μ .

Finally, we compute the gradient information with the following FOM-based formula:

$$(26) \quad \nabla_\mu \hat{\mathcal{J}}_h^{\text{loc}}(\mu) = \partial_\mu \mathcal{J}(u_{H,\ell,\mu}, \mu) + \partial_\mu r_\mu^{\text{pr}}(u_{H,\ell,\mu})[p_{H,\ell,\mu}].$$

We emphasize again that we do not use $u_{H,\ell,\mu}^{\text{ms}} \in V_{H,\ell,\mu}^{\text{ms}}$ and $p_{H,\ell,\mu}^{\text{ms}} \in V_{H,\ell,\mu}^{\text{ms}}$ but instead their coarse-scale representations $u_{H,\ell,\mu} \in V_H$ and $p_{H,\ell,\mu} \in V_H$ to be able to discard corrector information directly after their computation. Instead, we need to sacrifice the potential gain of accuracy. Note that we could still plugin $u_{H,\ell,\mu}^{\text{ms}} \in V_{H,\ell,\mu}^{\text{ms}}$ at some places in the formula, e.g., for the linear terms of \mathcal{J} since the related terms can be prepared simultaneously to the assembly of $\mathbb{K}_{T,\mu}$.

For keeping the theory short, we do not consider Hessian information in the localized approach but note that using Newton's method is relatively straightforward.

A priori error result of the PG-LOD Writing the solution of (19) as $u_{H,\ell,\mu}^{\text{ms}} = u_{H,\ell,\mu} - \mathcal{Q}_{\ell,\mu}(u_{H,\ell,\mu})$ with $u_{H,\ell,\mu} \in V_H$, we have the following a priori estimate, which was first shown in [24].

Theorem 4.1 (A priori convergence result for the PG-LOD). *For a fixed parameter $\mu \in \mathcal{P}$, let $u_{h,\mu} \in V_h$ be the finite-element solution of (P.b) given by*

$$a_\mu(u_{h,\mu}, v_h) = l(v_h) \quad \text{for all } v_h \in V_h.$$

Then, it holds that

$$\|u_{h,\mu} - u_{H,\ell,\mu}\|_{L^2} + \|u_{h,\mu} - u_{H,\ell,\mu}^{\text{ms}}\|_1 \lesssim (H + \theta^k \ell^{d/2}) \|f\|_{L^2(\Omega)},$$

with $0 < \theta < 1$ independent of H and ℓ , but dependent on the contrast $\kappa = \beta/\alpha$.

Although our setting is slightly different from the one in [24] (in terms of localization and interpolation), the proof can still be followed analogously. For a detailed discussion on the decay variable θ , we refer to [28, 29, 43]. We emphasize that the LOD is generally vulnerable to high-contrast problems or rapid coarse-scale changes induced by high conductivity channels since θ depends on the contrast of the problem. For neglecting the issue of high contrast in the LOD, the interpolation operator I_H has to be adjusted. Works in this direction have been made in [28, 13, 55], for instance. Note that using a right-hand-side correction as in [27, 29], for instance, can further enhance Theorem 4.1 but require additional corrector problems.

Remark 4.2 (Fulfillment of Assumption 3). *To fulfill Assumption 3, we may thus assume that an appropriate choice of the coarse-mesh size H , localization parameter ℓ , and the fine mesh size h is made to cope with the underlying problem. For the LOD, this aligns to fulfill the a priori result of Theorem 4.1 sufficiently well, i.e. that the errors $\|u_{h,\mu} - u_{H,\ell,\mu}\|_{L^2}$, $\|u_{h,\mu} - p_{H,\ell,\mu}\|_{L^2}$, and the corresponding H^1 -errors are sufficiently small. Further, with Assumption 4, we ruled out the concern that the dual problem may not fit to (19) in terms of accuracy.*

4.2 Localized reduced-order model using the TSRBLOD

It remains to explain the reduced-order model for the LOD-based optimality system. A particularly suitable localized RB model is the TSRBLOD, which has been recently introduced in [41]. The TSRBLOD can be divided into two reduction processes. In Stage 1, RB models for the corrector problems are constructed, and in Stage 2, these RB correctors are combined to a reduced two-scale formulation to reduce the global LOD scheme to a single reduced model. The idea of reducing the corrector problems similar to Stage 1 has already been proposed as RBLOD in [6]. While, in [41], the TSRBLOD showed to be more beneficial in terms of online efficiency, the additional coarse-scale reduction introduces an additional approximation error. According to the estimator study in [41], the additional error of the TSRBLOD can rigorously be controlled. As demonstrated in [41], for large coarse systems, the online-acceleration w.r.t. the RBLOD can be multiple orders of magnitude. On the other hand, the offline construction cost of the TSRBLOD is higher than the RBLOD since an additional offline-online decomposition is to be performed. In order to avoid an overload of methods, in this paper, we only consider the TSRBLOD for the TR-LRB method but mention that the same ideas can immediately be transferred to the RBLOD.

In Stage 1 of the TSRBLOD reduction process, we construct reduced corrector problems for each T , parameterized towards the respective FE shape functions on T . Based on Stage 1, we form a reduced two-scale space

$$\mathfrak{V}^{\text{rblo}} := V_H \oplus V_{\ell,T_1}^{\text{f,rb}} \oplus \cdots \oplus V_{\ell,T_{|\mathcal{T}_H|}}^{\text{f,rb}} \subset \mathfrak{V}.$$

Subsequently, we perform the second stage of our two-scale reduction. Since the primal and dual equations have different right-hand sides, we consider two different two-scale reduced spaces $\mathfrak{V}^{\text{rb,pr}}, \mathfrak{V}^{\text{rb,du}} \subset \mathfrak{V}^{\text{rb,loc}}$. Reducing the primal equation (20), given $\mathfrak{V}^{\text{rb,pr}}$, means to compute the two-scale reduced primal solution $\mathfrak{u}_\mu^{\text{rb}} \in \mathfrak{V}^{\text{rb,pr}}$ by

$$(27) \quad \mathfrak{u}_\mu^{\text{rb}} := \operatorname{argmin}_{\mathfrak{u} \in \mathfrak{V}^{\text{rb,pr}}} \sup_{\mathfrak{v} \in \mathfrak{V}} \frac{\mathfrak{F}_\mu(\mathfrak{v}) - \mathfrak{B}_\mu(\mathfrak{u}, \mathfrak{v})}{\|\mathfrak{v}\|_1}.$$

Further, let $u_{H,\ell,\mu}^{\text{rb}} \in V_H$ denote the resulting TSRBLOD coarse-scale approximation, which can be reconstructed from $\mathfrak{u}_\mu^{\text{rb}}$, just by using the V_H -part of the respective basis of $\mathfrak{V}^{\text{rb,pr}}$. Then, we define the corresponding reduced functional by

$$(28) \quad \hat{\mathcal{J}}_r^{\text{loc}}(\mu) := \mathcal{J}(u_{H,\ell,\mu}^{\text{rb}}, \mu).$$

Given the dual two-scale reduced space $\mathfrak{V}^{\text{rb,du}}$, the dual problem can be defined analogously to the construction of the TSRBLOD, with the vital difference that the right-hand side of the Stage 2 FOM system needs to be adjusted with the one from the dual problem. To be precise, we define

$$(29) \quad \mathfrak{F}_{\mu, u_{H,\ell,\mu}^{\text{rb}}}^{\text{du}} \left((v_H, v_{T_1}^f, \dots, v_{T_{|\mathcal{T}_H|}}^f) \right) := \partial_u \mathcal{J}(u_{H,\ell,\mu}^{\text{rb}}, \mu)[v_H].$$

By replacing \mathfrak{F} by $\mathfrak{F}_{\mu, u_{H,\ell,\mu}^{\text{rb}}}^{\text{du}}$ from (24) in (27) and using $\mathfrak{V}^{\text{rb,du}}$ instead, we obtain the two-scale dual solution $\mathfrak{p}_\mu^{\text{rb}} \in \mathfrak{V}^{\text{rb,du}}$ by

$$(30) \quad \mathfrak{p}_\mu^{\text{rb}} := \operatorname{argmin}_{\mathfrak{p} \in \mathfrak{V}^{\text{rb,du}}} \sup_{\mathfrak{v} \in \mathfrak{V}} \frac{\mathfrak{F}_{\mu, u_{H,\ell,\mu}^{\text{rb}}}^{\text{du}}(\mathfrak{v}) - \mathfrak{B}_\mu(\mathfrak{p}, \mathfrak{v})}{\|\mathfrak{v}\|_1},$$

which again uses the fact that a_μ is symmetric. With the resulting coarse approximation $p_{H,\ell,\mu}^{\text{rb}} \in V_H$ reconstructed from $\mathfrak{p}_\mu^{\text{rb}}$, we can compute the reduced gradient as

$$(31) \quad \nabla_\mu \hat{\mathcal{J}}_r^{\text{loc}}(\mu) = \partial_\mu \mathcal{J}(u_{H,\ell,\mu}^{\text{rb}}, \mu) + \partial_\mu r_\mu^{\text{pr}}(u_{H,\ell,\mu}^{\text{rb}})[p_{H,\ell,\mu}^{\text{rb}}].$$

Remark 4.3 (Generalization of the TSRBLOD approach to parameterized right-hand sides). *For carrying out the reduction process in this chapter, we emphasize that this requires generalizing the TSRBLOD approach to parameterized right-hand sides and output functionals. Thus, the offline-online decomposition as explained in [41] changes slightly. We still omit a further technical description for brevity, noting that the online efficiency remains the same.*

4.3 A posteriori error estimate for the reduced functional

Having set up the localized FOM and ROM approximation schemes, we aim at deriving the error estimator $\Delta_{\hat{\mathcal{J}}_r^{\text{loc}}}$ of the reduced functional, which is needed for characterizing the TR in (9). Luckily, the a posteriori result from [41] can directly be utilized for the two-scale formulations of the primal and dual systems. On top of that, similar to the a posteriori result in [39, 56], we combine a primal and dual estimate to obtain an estimator for the reduced functional. To this end, we use the following norms to assess the approximation quality of the two-scale approach:

$$\begin{aligned} \|\mathfrak{u}\|_{a,\mu}^2 &:= \|u_H - \sum_{T \in \mathcal{T}_H} u_T^f\|_{a,\mu}^2 + \rho \sum_{T \in \mathcal{T}_H} \|\mathcal{Q}_{\ell,\mu}^T(u_H) - u_T^f\|_{a,\mu}^2, \\ \|\mathfrak{u}\|_{1,\mu}^2 &:= \|u_H\|_1^2 + \rho \sum_{T \in \mathcal{T}_H} \|\mathcal{Q}_{\ell,\mu}^T(u_H) - u_T^f\|_1^2. \end{aligned}$$

Proposition 4.4 (Upper bound on the local primal model reduction error). *For $\mu \in \mathcal{P}$, let $\mathbf{u}_\mu \in \mathfrak{V}$ be the solution of (20). Let $\mathbf{u}_\mu^{rb} \in \mathfrak{V}^{rb}$ be the two-scale reduced solution of (27). Then, it holds*

$$(32) \quad \|\mathbf{u}_\mu - \mathbf{u}_\mu^{rb}\|_{a,\mu} \leq \Delta_{\text{pr}}^{rb}(\mu) := \eta_{a,\mu}(\mathbf{u}_\mu^{rb}),$$

with

$$(33) \quad \eta_{a,\mu}^{\text{pr}}(\mathbf{u}) := \sqrt{5}(\gamma_\ell^{pg})^{-1} \sup_{v \in \mathfrak{V}} \frac{\mathfrak{F}_\mu(v) - \mathfrak{B}_\mu(\mathbf{u}, v)}{\|v\|_1}.$$

Proof. The assertion follows directly from [41], exploiting the inf-sup stability of the two-scale equation. \square

Remark 4.5 (Equivalence of the two-scale norms). *Due to the definitions of $\|\cdot\|_{a,\mu}$, $\|\cdot\|_1$, $\|\cdot\|_{a,\mu}$, and $\|\cdot\|_1$ and the equivalences of $\|\cdot\|_{a,\mu}$ and $\|\cdot\|_1$, as well as $\|\cdot\|_{a,\mu}$, and $\|\cdot\|$, respectively, we note that the fine-scale errors $\|u_{H,\ell,\mu}^{ms} - u_{H,\ell,\mu}^{ms,rb}\|_{a,\mu}$, $\|u_{H,\ell,\mu}^{ms} - u_{H,\ell,\mu}^{ms,rb}\|$, and the coarse-scale errors $\|u_{H,\ell,\mu} - u_{H,\ell,\mu}^{rb}\|_{a,\mu}$, and $\|u_{H,\ell,\mu} - u_{H,\ell,\mu}^{rb}\|$ can be bounded by Δ_{pr}^{rb} with the respective equivalence constants, cf. [41].*

A similar result is also available for the equivalent μ -dependent $\|\cdot\|_1$ -norm.

The corresponding dual estimates account for the fact that the right-hand side contains the reduced primal solution instead of the true LOD solution.

Proposition 4.6 (Upper bound on the local dual model reduction error). *For $\mu \in \mathcal{P}$ let $\mathbf{p}_\mu \in \mathfrak{V}$ be the solution of the two-scale dual equation (25). Let $\mathbf{p}_\mu^{rb} \in \mathfrak{V}^{rb}$ be the two-scale reduced dual solution of (30). Then, it holds*

$$(34) \quad \|\mathbf{p}_\mu - \mathbf{p}_\mu^{rb}\|_{a,\mu} \leq \Delta_{\text{du}}^{rb}(\mu) := \frac{\sqrt{5}}{\gamma_k} (2\gamma_{k,\mu} \Delta_{\text{pr}}^{rb}(\mu) + \eta_{a,\mu}^{\text{du}}(\mathbf{p}_\mu^{rb})),$$

where $\eta_{a,\mu}^{\text{du}}$ is analogously defined as $\eta_{a,\mu}^{\text{pr}}$ but associated with (25).

Proof. We use the shorthands $\mathbf{e}_\mu^{\text{du}} := \mathbf{p}_\mu - \mathbf{p}_\mu^{rb} \in \mathfrak{V}^{rb}$ and $e_{H,\mu}^{\text{pr}} := u_{H,\ell,\mu} - u_{H,\ell,\mu}^{rb}$, where $u_{H,\ell,\mu} \in V_H$ and $u_{H,\ell,\mu}^{rb}$ are the V_H parts of \mathbf{u}_μ and \mathbf{u}_μ^{rb} , respectively. With the inf-sup stability of Equation (23), we have

$$\begin{aligned} \gamma_k / \sqrt{5} \|\mathbf{e}_\mu^{\text{du}}\|_{a,\mu} &\leq \sup_{0 \neq v \in \mathfrak{V}} \frac{\mathfrak{B}_\mu(\mathbf{e}_\mu^{\text{du}}, v)}{\|v\|_1} = \sup_{0 \neq v \in \mathfrak{V}} \left(\frac{\mathfrak{F}_{\mu,u_{H,\ell,\mu}}^{\text{du}}(v) - \mathfrak{B}_\mu(\mathbf{p}_\mu^{rb}, v)}{\|v\|_1} \right) \\ &= \sup_{0 \neq v \in \mathfrak{V}} \left(\frac{\mathfrak{F}_{\mu,u_{H,\ell,\mu}}^{\text{du}}(v)}{\|v\|_1} - \frac{\mathfrak{F}_{\mu,u_{H,\ell,\mu}^{rb}}^{\text{du}}(v)}{\|v\|_1} + \frac{\mathfrak{F}_{\mu,u_{H,\ell,\mu}^{rb}}^{\text{du}}(v)}{\|v\|_1} - \frac{\mathfrak{B}_\mu(\mathbf{p}_\mu^{rb}, v)}{\|v\|_1} \right) \\ &\leq 2\|k_\mu\| \|e_{H,\mu}^{\text{pr}}\| + \eta_{a,\mu}^{\text{du}}(\mathbf{p}_\mu^{rb}), \end{aligned}$$

with $\mathfrak{F}_{\mu,*}^{\text{du}}$ defined in (24), (29) which is linear in its sub-index argument due to the definition of J in (P.a). We attain the desired result utilizing Proposition 4.4 and Remark 4.5. \square

Similar to Remark 4.5, we note that the respective dual estimators can also bound the corresponding dual norms from Proposition 4.6. Finally, we derive the a posteriori error result for the reduced objective functional.

Proposition 4.7 (Upper bound for the reduced functionals). *For $\mu \in \mathcal{P}$ let $\mathbf{u}_\mu \in \mathfrak{V}$ be the two-scale solution of (20) with coarse part $u_{H,\ell,\mu} \in V_H$ and LOD-space representation $u_{H,\ell,\mu}^{ms} \in V_{H,\ell,\mu}^{ms}$. Further, let $\mathbf{p}_\mu \in \mathfrak{V}$ be the two-scale solution of (25) with coarse part $p_{H,\ell,\mu} \in V_H$ and LOD-space representation $p_{H,\ell,\mu}^{ms} \in V_{H,\ell,\mu}^{ms}$.*

(i) We have for the TSRBLOD reduced cost functional

$$|\hat{\mathcal{J}}_h^{loc}(\mu) - \hat{\mathcal{J}}_r^{loc}(\mu)| \lesssim \Delta_{\hat{\mathcal{J}}_r^{loc}}(\mu) := \Delta_{\text{pr}}^{rb}(\mu) \eta_{a,\mu}^{\text{du}}(\mathfrak{p}_\mu^{rb}) + (\Delta_{\text{pr}}^{rb}(\mu))^2 \gamma_{k_\mu} + \Delta_{trunc}^{rb}(\mu),$$

where $\mathfrak{p}_\mu^{rb} \in \mathfrak{V}^{rb,du}$ denotes the two-scale reduced dual equation and $\Delta_{trunc}^{rb}(\mu)$ is a truncation-reduction-based homogenization term which is specified below.

(ii) The truncation-reduction-based homogenization term $\Delta_{trunc}^{rb}(\mu)$ is defined as

$$(35) \quad \Delta_{trunc}^{rb}(\mu) := a_\mu(e_{H,\ell}^{\text{ms}}, \mathcal{Q}_{\ell,\mu}^{\text{rb}}(p_{H,\ell,\mu}^{rb}))$$

and can be estimated by

$$(36) \quad |\Delta_{trunc}^{rb}(\mu)| \leq \Delta_{\text{pr}}^{rb}(\mu) \left(2c \ell^{d/2} \theta^k \|p_{H,\ell,\mu}^{rb}\|_1 + \eta_{a,\mu}^{\text{du}}(\mathfrak{p}_\mu^{rb}) \right) + \alpha^{-1/2} \|p_{H,\ell,\mu}^{rb}\|_1 \eta_{a,\mu}^{\text{pr}}(\mathfrak{u}_\mu^{rb}),$$

with respective coarse- and two-scale-space primal and dual solutions and constant $c > 0$.

Proof. We utilize Assumption 4 to incorporate the estimates of Proposition 4.4 and Proposition 4.6. By using the shorthands $e_{H,\ell}^{\text{ms}} := u_{H,\ell,\mu}^{\text{ms}} - u_{H,\ell,\mu}^{\text{rb}}$ and $e_{H,\ell} := u_{H,\ell,\mu} - u_{H,\ell,\mu}^{\text{rb}}$, we have

$$\begin{aligned} |\hat{\mathcal{J}}_h^{loc}(\mu) - \hat{\mathcal{J}}_r^{loc}(\mu)| &= |\mathcal{J}(u_{H,\ell,\mu}, \mu) - \mathcal{J}(u_{H,\ell,\mu}^{\text{rb}}, \mu)| \\ &= |\mathcal{J}(e_{H,\ell}^{\text{ms}} + k_\mu(u_{H,\ell,\mu}, u_{H,\ell,\mu}) - k_\mu(u_{H,\ell,\mu}^{\text{rb}}, u_{H,\ell,\mu}^{\text{rb}}) \\ &\quad - a_\mu(e_{H,\ell}^{\text{ms}}, p_{H,\ell,\mu}^{\text{ms},\text{rb}}) + a_\mu(e_{H,\ell}^{\text{ms}}, p_{H,\ell,\mu}^{\text{ms},\text{rb}})| \\ &= |r_\mu^{\text{du}}(u_{H,\ell,\mu}^{\text{rb}}, p_{H,\ell,\mu}^{\text{ms},\text{rb}})[e_{H,\ell}^{\text{ms}}] + k_\mu(e_{H,\ell}^{\text{ms}}, e_{H,\ell}^{\text{ms}}) + a_\mu(e_{H,\ell}^{\text{ms}}, p_{H,\ell,\mu}^{\text{ms},\text{rb}})| \\ &\leq \eta_{a,\mu}^{\text{du}}(\mathfrak{p}_\mu^{rb}) \|e_{H,\ell}^{\text{ms}}\| + \gamma_{k_\mu} \|e_{H,\ell}^{\text{ms}}\|^2 + |a_\mu(e_{H,\ell}^{\text{ms}}, \mathcal{Q}_{\ell,\mu}^{\text{rb}}(p_{H,\ell,\mu}^{rb}))|, \end{aligned}$$

where we have used that

$$a_\mu(e_{H,\ell}^{\text{ms}}, p_{H,\ell,\mu}^{\text{ms},\text{rb}}) = -a_\mu(e_{H,\ell}^{\text{ms}}, \mathcal{Q}_{\ell,\mu}^{\text{rb}}(p_{H,\ell,\mu}^{rb})).$$

For (iii), we further note that

$$\begin{aligned} a_\mu(e_{H,\ell}^{\text{ms}}, \mathcal{Q}_{\ell,\mu}^{\text{rb}}(p_{H,\ell,\mu}^{rb})) &= a_\mu(e_{H,\ell}^{\text{ms}}, \mathcal{Q}_\mu(p_{H,\ell,\mu}^{rb})) \\ &\quad - a_\mu(e_{H,\ell}^{\text{ms}}, (\mathcal{Q}_\mu - \mathcal{Q}_{\ell,\mu} + \mathcal{Q}_{\ell,\mu} - \mathcal{Q}_{\ell,\mu}^{\text{rb}})(p_{H,\ell,\mu}^{rb})) \end{aligned}$$

and

$$\begin{aligned} a_\mu(e_{H,\ell}^{\text{ms}}, \mathcal{Q}_\mu(p_{H,\ell,\mu}^{rb})) &= \\ a_\mu((\mathcal{Q}_{\ell,\mu} - \mathcal{Q}_\mu)(u_{H,\ell,\mu} - u_{H,\ell,\mu}^{\text{rb}}) + (\mathcal{Q}_{\ell,\mu} - \mathcal{Q}_{\ell,\mu}^{\text{rb}})(u_{H,\ell,\mu}^{\text{rb}}), \mathcal{Q}_\mu(p_{H,\ell,\mu}^{rb})). \end{aligned}$$

We thus obtain

$$\begin{aligned} &|a_\mu(e_{H,\ell}^{\text{ms}}, \mathcal{Q}_{\ell,\mu}^{\text{rb}}(p_{H,\ell,\mu}^{rb}))| \\ &\leq \|e_{H,\ell}^{\text{ms}}\|_{a,\mu} (\|(\mathcal{Q}_\mu - \mathcal{Q}_{\ell,\mu})(p_{H,\ell,\mu}^{rb})\|_{a,\mu} + \|(\mathcal{Q}_{\ell,\mu} - \mathcal{Q}_{\ell,\mu}^{\text{rb}})(p_{H,\ell,\mu}^{rb})\|_{a,\mu}) \\ &\quad + \|\mathcal{Q}_\mu(p_{H,\ell,\mu}^{rb})\|_{a,\mu} (\|(\mathcal{Q}_\mu - \mathcal{Q}_{\ell,\mu})(e_{H,\ell})\|_{a,\mu} + \|(\mathcal{Q}_{\ell,\mu} - \mathcal{Q}_{\ell,\mu}^{\text{rb}})(u_{H,\ell,\mu}^{\text{rb}})\|_{a,\mu}) \\ &\lesssim \Delta_{\text{pr}}^{rb}(\mu) (k^{d/2} \theta^k \|p_{H,\ell,\mu}^{rb}\|_{a,\mu} + \eta_{a,\mu}(\mathfrak{p}_\mu^{rb})) + \|p_{H,\ell,\mu}^{rb}\|_{a,\mu} (k^{d/2} \theta^k \|e_{H,\ell}\|_{a,\mu} + \eta_{a,\mu}(\mathfrak{u}_\mu^{rb})) \\ &\leq \Delta_{\text{pr}}^{rb}(\mu) \left(2k^{d/2} \theta^k \|p_{H,\ell,\mu}^{rb}\|_{a,\mu} + \eta_{a,\mu}^{\text{du}}(\mathfrak{p}_\mu^{rb}) \right) + \|p_{H,\ell,\mu}^{rb}\|_{a,\mu} \eta_{a,\mu}^{\text{pr}}(\mathfrak{u}_\mu^{rb}), \end{aligned}$$

where we have used the a priori result on the corrector decay (cf. Theorem 4.1) and Remark 4.5. Using the equivalence of $\|\cdot\|_{a,\mu}$ and $\|\cdot\|_1$ attains the assertion. \square

Remark 4.8 (Truncation-reduction-based homogenization term). *We emphasize that, in Proposition 4.7, we intentionally separated the error estimation from the homogenization term $\Delta_{trunc}^{rb}(\mu)$, and presented a rather naive estimation of it. The reason is that the term can be interpreted as a truncation term that (without reduction) vanishes for true LOD-space functions, i.e.*

$$(37) \quad a_\mu(u_{H,\mu}^{ms}, \mathcal{Q}_\mu(p_{H,\ell,\mu}^{rb})) = 0,$$

for all $u_{H,\mu}^{ms} \in V_{H,\mu}^{ms}$, since $\mathcal{Q}_\mu(p_{H,\ell,\mu}^{rb}) \in V_h^f$ and $V_h = V_{H,\mu}^{ms} \oplus_{a_\mu} V_h^f$. Due to Assumption 3, we further note that the a priori term can be neglected from (36), such that Δ_{trunc}^{rb} can be computed efficiently.

The computation of the above-explained estimators can be offline-online decomposed with a numerically stable procedure, which has carefully been explained in [41]. However, while the additional orthonormalization of the residual terms of Stage 1 is necessary for the Stage 2 residual, the additional expenses for stabilizing the Stage 2 residual is not strictly needed in our approach. Indeed, concerning the overall cost of the TR-LRB algorithm, we omit the offline-online decomposition of Stage 2 entirely and instead compute the residual and its Riesz-representative whenever needed, cf. Section 4.5.

4.4 Local basis enrichment

It remains to explain the adaptive localized enrichment strategy for a parameter $\mu \in \mathcal{P}$, for instance, a newly accepted iterate $\mu^{(k)} \in \mathcal{P}$ of the TR-LRB algorithm. In [9], it is discussed that we can either update the RB space unconditionally or optionally w.r.t. some enrichment flag. For local RB models, the situation is more complex. While we, at least for obtaining certified convergence in the sense of Theorem 3.1, always perform an enrichment, some local models may reject or dismiss the snapshots if, e.g., the selected parameter does not influence the local model. For this reason, a localization of the error result is crucial since we may employ the local error estimators for the local models to decide whether an update is required. Such a strategy is also commonly known as adaptive online enrichment.

First of all, we note that the estimates $\eta_{a,\mu}^{\text{pr}}$ and $\eta_{a,\mu}^{\text{du}}$ can indeed be boiled down to their respective local reduction errors, namely the standard RB estimation of Stage 1 of the reduction process for the TSRBLOD, see [41] for a clarification. In detail, for each $T \in \mathcal{T}_H$, we use the residual-norm based estimate

$$(38) \quad \|\mathcal{Q}_{\ell,\mu}^T(v_H) - \mathcal{Q}_{\ell,\mu}^{T,rb}(v_H)\|_{a,\mu} \leq \eta_{T,\mu}(\mathcal{Q}_{\ell,\mu}^{T,rb}(v_H)),$$

where

$$(39) \quad \eta_{T,\mu}(\mathcal{Q}_{\ell,\mu}^{T,rb}(v_H)) := \alpha^{-1/2} \sup_{v_T^f \in V_{h,\ell,T}^f} \frac{a_\mu^T(v_H, v_T^f) - a_\mu(\mathcal{Q}_{\ell,\mu}^{T,rb}(v_H), v_T^f)}{\|v_T^f\|_1}.$$

For the TR-LRB scheme, at an enrichment point, for every T , we use the Stage 1 estimator $\Delta_{\text{loc}}^T(\mu) := \eta_{T,\mu}(\mathcal{Q}_{\ell,\mu}^{T,rb}(v_H))$ to decide for a local enrichment. If the estimator is below a specific tolerance $\tau_{\text{loc}} > 0$, i.e.

$$(40) \quad \Delta_{\text{loc}}^T(\mu) \leq \tau_{\text{loc}},$$

the enrichment is skipped. For a sufficiently small τ_{loc} , the enrichment strategy can be considered unconditionally. However, the computational effort can still decrease significantly, e.g., if a local modal is not associated with the parameter. We also note that the online adaptive approach is also motivated by the numerical experiments in [41, 6], where it was demonstrated that moderate choices of τ_{loc} already produce acceptable reduced models. However, it is clear that the choice of the tolerance τ_{loc} is highly problem dependent. If the tolerance is chosen too large, the method could be stagnant (due to the missing local basis quality). In such cases, it is recommended to refine the tolerance adaptively. For simplicity we omit such a strategy in this paper.

While the local enrichment is helpful for the Stage 1 reduction, another crucial question is how the Stage 2 reduction is performed afterwards. Note that the TSRBLOD model is based on the reduced models from Stage 1, meaning that, whenever the Stage 1 models are enriched, the Stage 2 reduction needs to be restarted from scratch. Thus, there is more freedom in choosing the enrichment parameters for the TSRBLOD model. With respect to the fact that, at iteration k , the Stage 1 models are exact (up to the tolerance τ_{loc}), we propose to enrich the TSRBLOD model for the same sequence of TR iterates $\mu^{(i)}$, for $i = 0, \dots, k$. Greedy-based enrichments of the TSRBLOD are also possible, mainly because the snapshot generation with Stage 1 is fast. However, our experiments suggested that greedy-search algorithms do not provide a significant update to the respective accuracy of the TSRBLOD model.

Let us also mention that we did not use optional local enrichment strategies for the R-TR-LRB algorithm since we do not assemble the estimators in the first iterations.

4.5 TR-TSRBLOD algorithm in Pseudo-code

For clarity, we summarize the (R)-TR algorithms for parameter optimization of multiscale problems in the following.

Algorithm 1: TR-TSRBLOD algorithm

Data: Initial TR radius $\delta^{(0)}$, TR shrinking factor $\beta_1 \in (0, 1)$, tolerance for enlarging the TR radius $\eta_\varrho \in [\frac{3}{4}, 1]$, initial parameter $\mu^{(0)}$, stopping tolerance for the sub-problem $\tau_{\text{sub}} \ll 1$, stopping tolerance for the first-order critical condition τ_{FOC} with $\tau_{\text{sub}} \leq \tau_{\text{FOC}} \ll 1$, safeguard for TR boundary $\beta_2 \in (0, 1)$, tolerance for online enrichment τ_{loc}

- 1 Initialize TSRBLOD model with $\mu^{(0)}$;
- 2 Set $k = 0$;
- 3 **while** $\|\mu^{(k)} - P_{\mathcal{P}}(\mu^{(k)} - \nabla_{\mu} \hat{\mathcal{J}}_h^{\text{loc}}(\mu^{(k)}))\|_2 > \tau_{\text{FOC}}$ **do**
- 4 Compute $\mu^{(k+1)}$ from (9) with termination criteria (10);
- 5 **if** *Sufficient decrease condition* (11) *is fulfilled* (cf. [39]) **then**
- 6 Accept $\mu^{(k+1)}$ and possibly enlarge the TR-radius (cf. [39]);
- 7 Before enrichment: check (12) for early termination;
- 8 // TSRBLOD enrichment
- 9 **Stage 1:** enrich the local RB corrector models at $\mu^{(k+1)}$ if (40) including pre-assembly of the local estimators Δ_{loc}^T ;
- 10 **Stage 2:** construct the primal and dual two-scale models and enrich for all $\mu^{(k')}$, $k' = 0, \dots, k + 1$, and do not pre-assemble $\Delta_{\hat{\mathcal{J}}_r^{\text{loc}}}$;
- 11 **else**
- 12 Reject $\mu^{(k+1)}$, shrink the TR radius $\delta^{(k+1)} = \beta_1 \delta^{(k)}$ and go to 4;
- 13 **end**
- 14 Set $k = k + 1$;
- 15 **end**

We emphasize that the TR-TSRBLOD procedure in Algorithm 1 is analog to the algorithm presented in [39] but with the major difference that the localized LOD-based FOM and the localized TSRBLOD reduced model including its respective estimator is used. The details of Algorithm 2 are explained in Section 3.2. As stated in Line 7 of Algorithm 1, we check the FOM termination criterion prior to the enrichment. This is because online enrichment, including the assembly of the respective estimators, is relatively more expensive than the pure computation of the termination criterion. A similar strategy is used in Line 9 of Algorithm 2. However, since Stage 1 is generally less expensive for the relaxed variant, we check the FOM-based termination criterion between Stage 1 and Stage 2 of the TSRBLOD.

We further note that in Lines 5 and 6 of both algorithms, we have neglected detailed information on the exact computational procedure concerning the cheap conditions for the sufficient decrease conditions

according to [60] and the enlarging of the TR-radius with a suitable accessible condition. For both features, we again refer to [39].

Algorithm 2: Relaxed TR-TSRBLOD algorithm

Data: Initial TR radius $\delta^{(0)}$, TR shrinking factor $\beta_1 \in (0, 1)$, tolerance for enlarging the TR radius $\eta_\varrho \in [\frac{3}{4}, 1)$, initial parameter $\mu^{(0)}$, stopping tolerance for the sub-problem $\tau_{\text{sub}} \ll 1$, stopping tolerance for the first-order critical condition τ_{FOC} with $\tau_{\text{sub}} \leq \tau_{\text{FOC}} \ll 1$, safeguard for TR boundary $\beta_2 \in (0, 1)$, relaxation sequences $(\varepsilon_{\text{TR}}^{(k)})_k$ and $(\varepsilon_{\text{cond}}^{(k)})_k$

- 1 Initialize TSRBLOD model with $\mu^{(0)}$;
- 2 Set $k = 0$;
- 3 **while** $\|\mu^{(k)} - P_{\mathcal{P}}(\mu^{(k)} - \nabla_{\mu} \hat{\mathcal{J}}_h^{\text{loc}}(\mu^{(k)}))\|_2 > \tau_{\text{FOC}}$ **do**
- 4 Compute $\mu^{(k+1)}$ from (14) with relaxed termination (10a) and (15);
- 5 **if** Relaxed sufficient decrease condition (16) is fulfilled (cf. [39]) **then**
- 6 Accept $\mu^{(k+1)}$ and possibly enlarge the TR-radius (cf. [39]);
- 7 // TSRBLOD enrichment
- 8 **Stage 1:** enrich the local RB corrector models at $\mu^{(k+1)}$ and skip offline assembly of the local estimators if $\varepsilon_{\text{TR}}^{(k)}$ is large enough;
- 9 Before Stage 2 enrichment: check (12) for early termination;
- 10 **Stage 2:** construct the primal and dual two-scale models and enrich for all $\mu^{(k')}$, $k' = 0, \dots, k+1$, and do not assemble estimator;
- 11 **else**
- 12 | Reject $\mu^{(k+1)}$, shrink the TR radius $\delta^{(k+1)} = \beta_1 \delta^{(k)}$ and go to 4;
- 13 **end**
- 14 Set $k = k + 1$;
- 15 **end**

5 Numerical experiments

We analyze the presented TR-LRB approaches with two experiments with the same problem description, only differing in their respective multiscale complexity. We define the fine-mesh by $n_h \times n_h$ and the coarse-mesh by $n_H \times n_H$ quadrilateral grid-blocks of $\Omega := [0, 1]^2$, used to determine the standard FE mesh \mathcal{T}_h and \mathcal{T}_H , respectively, with traditional \mathcal{P}^1 -FE spaces V_h and V_H . The mesh-sizes h and H can be computed from n_h and n_H . In the first small experiment, we compare the localized methods to FEM-based (TR-RB) methods, whereas, in the second large experiment, we neglect FEM entirely, as it is computationally infeasible.

In the experiments, we mainly focus on the number of evaluations relative to their complexity to the fine FEM mesh-size h , the coarse LOD mesh-size H , or the respective low RB dimensions of the reduced models. Moreover, we provide run time comparisons that hint at the computational efficiency observed with our specific implementation.

We emphasize that our computations were performed on an HPC cluster with 400 parallel processes. Nevertheless, the observed run times can not be interpreted as minimal computational times of the localized algorithms. More HPC-based and non-Python-based implementations can strengthen the localized approaches even more. We further emphasize that the Stage 2 reduction has been implemented as a serialized process that neither gathers the observed data from Stage 1 efficiently nor uses the sparsity pattern of the two-scale system matrix to a minimal extent.

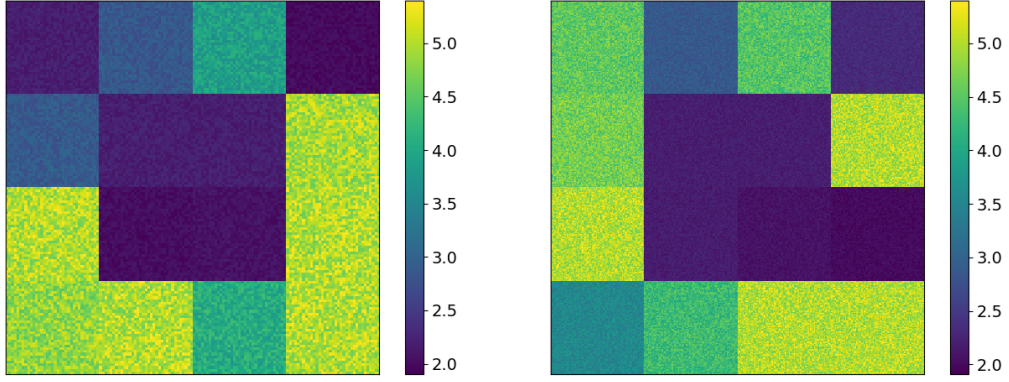


Figure 1: Coefficient A_μ^1 with $N_1 = 150$ (left) and A_μ^2 with $N_2 = 300$ (right) for the desired state of $\mu^d \in \mathcal{P}$.

In our numerical experiment, we use the L^2 -misfit objective functional with a Tikhonov-regularization term, i.e.

$$\mathcal{J}(v, \mu) = \frac{\sigma_d}{2} \int_D (I_H(v) - u^d)^2 \, dx + \frac{1}{2} \sum_{i=1}^P \sigma_i (\mu_i - \mu_i^d)^2 + 1.$$

Here, $\mu^d \in \mathcal{P}$ is the desired parameter and $u^d = I_H(u_{\mu^d})$ the corresponding desired solution specified in each experiment. The use of the interpolation operator I_H ensures Assumption 4. Moreover, using an actual solution as desired temperature and the respective desired parameter in the objective functional ensures that the optimization problem is sufficiently regular, such that all optimization methods converge to the same point. We note that \mathcal{J} can easily be written in the linear-quadratic form as in (P.a), cf. [39]. For the diffusion or conductivity coefficient A_μ in the symmetric bilinear form a_μ , we consider a 4x4-thermal block problem with two different thermal block multiscale coefficients A_μ^1 and A_μ^2 , i.e.

$$A_\mu = \sum_{\xi=1}^{16} \mu_\xi A_\mu^{1,\xi} + \sum_{\xi=17}^{32} \mu_\xi A_\mu^{2,\xi}.$$

Each of the 4x4 blocks has its linear parameter value, i.e., $\mathcal{P} \subseteq \mathbb{R}^{32}$. The respective parameterized multiscale blocks are given by $A_\mu^{1,\xi} = A_\mu^1|_{\Omega_{i,j}}$ and $A_\mu^{2,\xi} = A_\mu^2|_{\Omega_{i,j}}$, where $\Omega_{i,j}$ denotes the (i,j) -th thermal block for $i, j = 1, 2, 3, 4$. The multiscale features are randomly constructed with normally distributed values in $\mathcal{N}([0.9, 1.1])$ on a $N_1 \times N_1$ (for A_μ^1) and $N_2 \times N_2$ (for A_μ^2) quadrilateral grid. The specific values for N_1 and N_2 are given for each experiment. Due to the affine decomposition of A_μ , the multiscale features are linearly scaled by μ_ξ within each thermal block. We would like to point out that the multiscale data does not admit periodicity or any other additional structure; see Figure 1 for a visualization. Moreover, both coefficients A_μ^1 and A_μ^2 have low-conductivity blocks in the middle of the domain, i.e., for $\Omega_{i,j}$, $i, j = 2, 3$. The low conductivity is enforced by a restriction on the parameter space, i.e. we consider the admissible parameter set $\mathcal{P} = [1, 4]^{24} \times [1, 1.2]^8$. We choose the non-parameterized constant function $f_\mu \equiv 10$ as right-hand-side function. As also used in [39], for the inner product of V_h , we use the energy norm $\|\cdot\| := \|\cdot\|_{a, \check{\mu}}$ for a fixed parameter $\check{\mu} \in \mathcal{P}$ in the middle of the parameter space. Thus, constants in the estimators can easily be deduced by the min/max-theta approach, cf. [39]. For the two-scale estimators, we further approximate the maximum contrast κ and the respective constants α and β accordingly.

Details on the fine- and coarse-mesh are given in the respective experiments. The desired parameter $\mu^d \in \mathcal{P}$ is equal for both experiments, and mimics the case where boundary constraints are active, i.e.

we set $\mu_i^d = 4$ for $i = 3, 4, 6, 7, 8, 9, 11, 14$ and $\mu_i^d = 1.2$ for $i = 28, 29, 30, 31$. The remaining values of μ^d are chosen randomly, see Figure 1. The initial guess $\mu^{(0)}$ is also chosen randomly, where we note that the choice of the initial guess is not relevant for the shown results, which is why we only show the experiments for a single initial guess. Furthermore, the weights for the objective functional are chosen as $\sigma_d = 100$ and $\sigma_i = 0.001$ for each $i = 1, \dots, P$.

Similar to the experiments in [39], we choose an initial TR radius of $\delta^0 = 0.1$, a TR shrinking factor $\beta_1 = 0.5$, an Armijo step-length $\kappa = 0.5$, a truncation of the TR boundary of $\beta_2 = 0.95$, a tolerance for enlarging the TR radius of $\eta_\varrho = 0.75$, a stopping tolerance for the TR sub-problems of $\tau_{\text{sub}} = 10^{-8}$, a maximum number of TR iteration $K = 40$, a maximum number of sub-problem iterations $K_{\text{sub}} = 400$, a maximum number of Armijo iteration of 50, and a stopping tolerance for the FOC condition $\tau_{\text{FOC}} = 10^{-6}$.

State-of-the-art methods The following algorithms are used to compare our algorithms to the literature.

- 1. FEM BFGS:** Similar to the work in [56, 39], we perform a standard projected BFGS method that is solely based on classical FEM evaluations. This means that the high-fidelity space V_h is used as the only approximation space, and no reduced approach is used.
- 2. TR-RB BFGS [39]:** Given the FEM discretization used for Method 1, we use a trust-region reduced basis algorithm with full certification and global RB evaluations based on FEM enrichments. As the reduced model, we choose the NCD-corrected approach with Lagrangian enrichment, cf. [39]. Moreover, we use the projected BFGS as the ROM-based TR sub-problem. As explained in Section 3, after each sub-problem, the global RB model is enriched after acceptance of the iterate, and the algorithm is terminated with a FEM-based FOC-type criterion.

Selected methods introduced in this paper This paper introduced a relaxation of the TR-(L)RB method and further proposed a localized approach tailored towards multiscale problems. We consider the following relaxed variant of Method 2:

- 2.r R-TR-RB BFGS:** In this method, we use the relaxed trust-region reduced basis variant for the FEM-based TR-RB algorithm, as explained above. We use global NCD-corrected RB evaluations with relaxed certification as explained in Section 3.2. For the relaxation, we choose the relaxation sequences $\varepsilon_{\text{TR}}^{(k)} = \varepsilon_{\text{cond}}^{(k)} := 10^{10-k}$. Therefore, the first iterations can be considered certification-free, and, as discussed in Section 3.2, we do not pre-assemble the TR-estimator for $k \leq 8$. Moreover, from iteration count $k > 27$, we relax the TR-RB method below double machine-precision and follow the TR-RB method in its original form.

As detailed in Section 4, given a respectively accurate LOD discretization, we formulate the following localized methods.

- 3. PG-LOD BFGS:** For comparison, we utilize the standard projected BFGS method with PG-LOD evaluations without using reduced models. The PG-LOD system is always constructed from scratch and does not use any prior knowledge from previous parameters. In particular, if FEM is not accessible and Assumption 3 is given, this method is considered as the FOM method.
- 4. TR-TSRBLOD BFGS:** We use the localized TSRBLOD reduction process as detailed in Section 4.2 for the PG-LOD and use the TR-LRB method with PG-LOD enrichments and local RB evaluations based on the TSRBLOD. The procedure is summarized in Algorithm 1. The sub-problems are again solved with the BFGS method, and the outer algorithm is fully certified. Moreover, we use a local enrichment tolerance $\tau_{\text{loc}} = 10^{-3}$ which has proven to be sufficient for our experiment, cf. Section 4.4.
- 4.r R-TR-TSRBLOD BFGS:** Just as explained in Method 2.r, we devise the relaxed version of Method 4., by choosing $\varepsilon_{\text{TR}}^{(k)} = \varepsilon_{\text{cond}}^{(k)} := 10^{10-k}$. Again, this means that the first iterations are

certification-free, and no error estimators need to be prepared. The procedure is summarized in Algorithm 2.

Complexity measures To assess the presented methods w.r.t. their computational demands, we count the evaluations of the respective systems. To be precise, we deviate between the following complexities:

FEM: FEM evaluations, proportional to \mathcal{T}_h , which are needed for approximating (P.b) or (6) with FEM or for enriching the respective global RB model for Methods 2.r and 2.

RB: Global RB evaluations for approximating the FEM system, proportional to the global basis size, used in Methods 2.r and 2.

LOD coarse: Coarse PG-LOD system evaluations with exact corrector data, meaning to solve (19) or (23), proportional to the coarse mesh \mathcal{T}_H . These are only required in Method 3 and for the FOM-based termination criterion in Methods 4.r and 4.

LOD local: Local evaluations of all FOM corrector problems that are required for assembling the multiscale stiffness matrix of (19) and (23), locally proportional to $U_\ell(T)_h$.

RBLOD coarse: Coarse PG-LOD system evaluations with RB-based corrector data for the multiscale stiffness matrix, required for the snapshots generation in the TSRBLOD, proportional to the coarse mesh \mathcal{T}_H .

RBLOD local: RB evaluations of the RB corrector problems, proportional to the local RB sizes.

TSRBLOD: RB evaluations of the TSRBLOD system, proportional to the two-scale RB size.

Error measures As the optimization target, we validate the respective accuracy of the methods by considering the relative error in the optimal value of $\hat{\mathcal{J}}$, i.e., we consider

$$e^{\hat{\mathcal{J}},\text{rel}}(\bar{\mu}) := |\hat{\mathcal{J}}(\mu^d) - \hat{\mathcal{J}}(\bar{\mu})| / \hat{\mathcal{J}}(\mu^d),$$

where $\bar{\mu}$ is the respective convergence point of the optimization methods and $\hat{\mathcal{J}}$ is either the FEM-based objective functional $\hat{\mathcal{J}}_h$ or the LOD-based objective functional $\hat{\mathcal{J}}_h^{\text{loc}}$.

5.1 Experiment 1: Moderately sized experiment for comparison with FEM-based methods

In what follows, we consider an experiment where FEM solves are computationally affordable. To this end, we set the resolution of the multiscale coefficients to $N_1 = 150$ and $N_2 = 300$. For the fine-mesh, we thus choose $n_h = 1200$ to ensure at least 4 quadrilateral grid cells in each of the rapidly varying multiscale features. Therefore, the FEM mesh has 1.4 Mio degrees of freedom. For the coarse-grid, we choose $n_H = 20$, which results in only 400 coarse grid cells and, in particular, $\ell = 3$ and 176.400 fine-mesh elements for full patches $U_\ell(T)$. Concerning, the objective functional, we compute u_{μ^d} as the FEM solution of (P.b) for μ^d .

We emphasize that for this experiment, Assumption 3 is not entirely fulfilled. Instead, an approximation error of the PG-LOD in $\hat{\mathcal{J}}$ at the desired parameter μ^d is still observable, and we have

$$|\hat{\mathcal{J}}_h^{\text{loc}}(\mu^d) - \hat{\mathcal{J}}_h(\mu^d)| = 8.25 \cdot 10^{-6}.$$

Although this violates Assumption 3, we can expect that all methods converge up to the LOD discretization error, which is sufficiently close for this experiment.

In Figure 2(left), we visualize the number of affine components of the local corrector models that are directly associated with the number of affine components in A_μ . Thus, the number of affine components can be determined by the number of thermal blocks that lie in the patch. The thermal blocks are

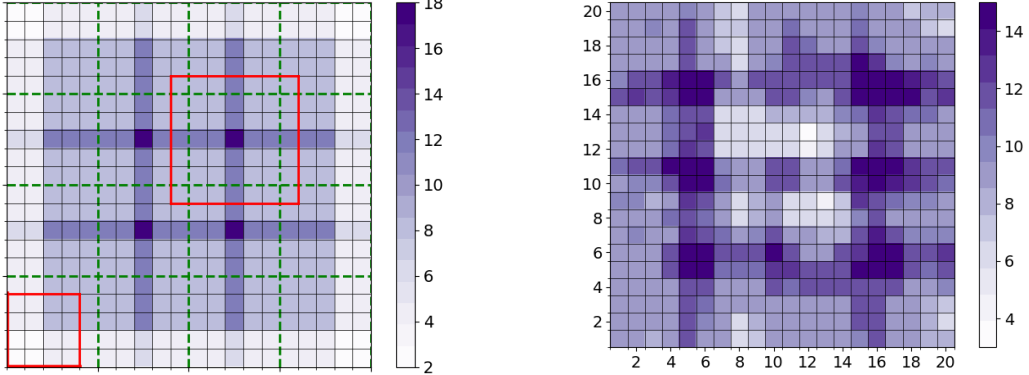


Figure 2: Left: Number of affine coefficients in each patch problem T for $n_H = 20$ and $\ell = 3$. The thermal block structure of $A_\mu^{1,\xi}$ and $A_\mu^{2,\xi}$ is highlighted in green, two patch instances are highlighted in red. Right: local corrector RB sizes of the Stage 1 models after successful termination of Method 4.

highlighted in green, and since $\ell = 3$, the resulting affine components can be counted in the plot. For instance, the lower-left element's patch only reaches the lower-left thermal block (resulting in 2 affine coefficients). Moreover, the elements that directly lie inside the inner thermal blocks have a patch that reaches up until all 9 neighboring blocks (resulting in 18 affine components each). The discussed patch instances are highlighted in red in Figure 2. We conclude that the corrector problems have a more minor parameter dependence than globalized RB methods. In turn, the local RB models can be expected to require less basis functions.

In Figure 2(right), the final local RB size of the Stage 1 models is depicted. It can be seen that the model requires a relatively rich space at the coarse elements that are close to the "jumps" in the desired parameter, cf Figure 1. As expected, the low conductivity blocks in the middle of the domain do not require many RB enrichments since the optimization problem in these blocks is less demanding. In addition, from solely looking at Figure 2(left), one would guess that the local patch problems that admit the highest number of affine components require the most basis functions. The fact that this expectation is not valid further proves that the optional enrichment plays a significant role in the algorithm.

We note that all compared methods indeed converged up to the chosen tolerance τ_{FOC} to the same point, and it was posteriorly verified that the point is indeed a local optimum. In Table 1 and Table 2, we report relevant information on the evaluation counts, the iteration, and the observed run times.

| Evaluations | | | LOD | | Stage 1 | | TS | | |
|-------------|------------|----------|------|---------------|---------|----------|------------|-------|--------|
| | FEM | RB | Coa. | Local | Coa. | Local | | O.it. | Time |
| Cost factor | h | N_{RB} | H | $U(T_H)_h$ | H | N_{RB} | N_{RB} | | |
| 1. FEM | 280 | - | - | - | - | - | - | 92 | 11402s |
| 2. TR-RB | 12 | 1546 | - | - | - | - | - | 5 | 1226s |
| 2.r R-TR-RB | 10 | 862 | - | - | - | - | - | 4 | 410s |
| 3. PG-LOD | - | - | 244 | 131200 | - | - | - | 80 | 620s |
| 4. TR-TS | - | - | 10 | 8000 | 30 | 48000 | 910 | 6 | 579s |
| 4.r R-TR-TS | - | - | 8 | 6400 | 30 | 48000 | 316 | 5 | 272s |

Table 1: Experiment 1: Evaluations and timings of selected methods

From Table 1, we conclude that all Methods 2-4 give a significant speedup to the standard FEM Method 1. Although 92 iterations of Method 1 and the corresponding 280 FEM evaluations are relatively few for a 32-dimensional optimization problem, the computational effort required to perform a FEM solution with 1.4 Mio. DoFs harm the speed of the method. As already shown in [39], the TR-RB Method 2 is mainly designed to avoid expensive FEM evaluations and converges already after 4 and 5 outer iterations, which only requires 12 and 10 FEM-based enrichments of the reduced spaces. On

| Method | Total | Speedup | Online | | Offline | | | $e^{\mathcal{J}_h, \text{rel}}$ |
|-------------|--------|---------|--------|-------|---------|---------|---------|---------------------------------|
| | | | outer | inner | FEM | Stage 1 | Stage 2 | |
| 1. FEM | 11402s | - | 11402s | - | - | - | - | 4.18e-10 |
| 2. TR-RB | 1226s | 9 | 41s | 3s | 1165s | - | - | 5.37e-11 |
| 2.r R-TR-RB | 410s | 28 | 34s | 4s | 348s | - | - | 7.75e-10 |
| 3. PG-LOD | 620s | 18 | 620s | - | - | - | - | 4.22e-06 |
| 4. TR-TS | 579s | 20 | 41s | 100s | - | 311s | 127s | 4.22e-06 |
| 4.r R-TR-TS | 272s | 42 | 4s | 4s | - | 193s | 71s | 4.22e-06 |

Table 2: Experiment 1: More details on run times and accuracy of selected methods

the other hand, the 1546 and 862 inner RB evaluations are cheap and do not harm the computational speed of the method.

As expected, the localized methods only converge until the priorly known approximation error of the PG-LOD is reached. However, it can be seen that the TR-LRB methods find the same point and are not subject to severe approximation issues.

A significant reason why the TSRBLOD method is particularly suitable in this work is its very efficient online phase. This result can be obtained by Table 2, where extended timings are given for the TSRBLOD method. Just as the efficient TR-RB methods, only a few seconds are required to solve the sub-problems in the relaxed variant, independent of the coarse LOD mesh. Instead, the sub-problem is more demanding for the fully certified variant, which goes back to the fact that we did not afford the offline time to reduce the respective error estimator in Stage 2.

It can further be noticed that the localized methods show a comparably good convergence speed w.r.t. the FEM based methods, although FEM is still comparably fast. We also see that Method 3, considered the localized FOM, shows a strong convergence speed. This is due to the relatively small patch problems such that the localized corrector problems and the corresponding Stage 2 reduction do not pay off massively.

The relaxed versions of the TR-(L)RB methods show a remarkably fast convergence behavior in this experiment. One reason for this is that the fully enforced certification cannot detect the full benefit from the surrogate model and, instead, truncates the sub-problems too early. With our choice of the relaxation parameters, the relaxed TR methods unconditionally trust the first surrogate models, allowing the overall algorithm to converge with fewer outer iterations. On top of that, the enrichment time is significantly lower, which goes back to the left-out pre-assembly of the error estimates.

In conclusion, FEM based-methods can reliably be replaced by localized methods already for moderately small fine-mesh sizes. However, the full benefit of the TR-LRB approaches can only be deduced for scenarios where the PG-LOD is costly in itself. Thus, in the second experiment, we increase the complexity of the multiscale structure of the problem.

5.2 Experiment 2: Large scale example

We consider a large scale example, where the global FEM mesh does not fit into the machine's memory. We set the multiscale resolution to $N_1 = 1.000$ and $N_2 = 250$. For the fine-mesh, we again aim to have at least 4 fine mesh entities in each multiscale cell and choose $n_h = 4000$. Therefore, the FEM mesh would have 16 Mio degrees of freedom, which can be considered prohibitively large. Hence, we do not utilize FEM-based methods and only compare Methods 3 and 4. For the coarse-grid, we choose $n_H = 40$, which results in 1600 coarse grid cells and, in particular, $\ell = 4$ and 810.000 fine-mesh elements for full patches $U_\ell(T)$. Since FEM evaluations are not available, the desired solution u_{μ^d} is computed with the PG-LOD, i.e. we solve (19) for μ^d .

Similar to the above illustrations, in Figure 3, we report the respective number of affine components of the patch problems as well as the final local RB sizes of the certified TR-TSRBLOD method with optional enrichment (Method 4). In particular, Figure 3 can be interpreted as the refined version of Figure 2, where it is even more visible that the local corrector problems have fewer affine components and need more basis functions for the corrector problems that are largely affected by the "jumps" in

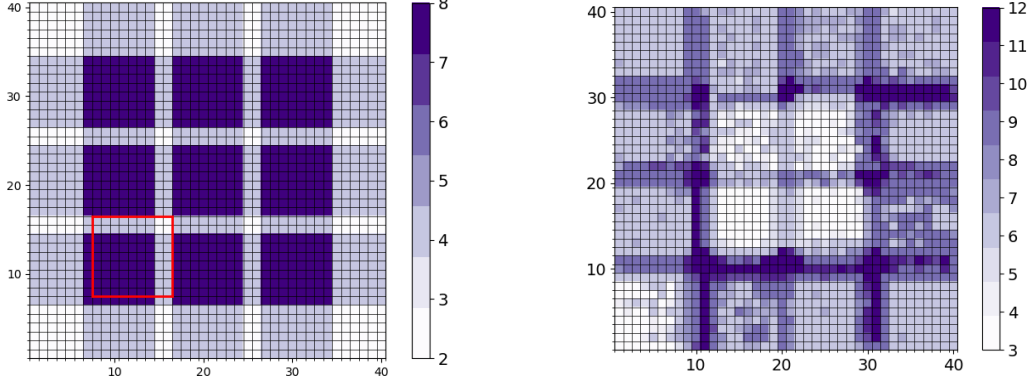


Figure 3: Left: Number of affine coefficients in each patch problem T for $n_H = 40$ and $\ell = 4$. One patch instance is highlighted in red. Right: local corrector RB sizes of the Stage 1 models after successful termination of Method 4.

the desired thermal block state, depicted in Figure 1. Just as before, it can be seen that the amount of basis functions is also associated with the intensity of the respective "jumps", and the low conductivity in the middle of the domain is well visible.

In Table 3 and Table 4, we again provide an extensive comparison concerning evaluations, run time, and iteration counts of the methods. It can be seen that the TSRBLOD-based methods successfully reduce the computational effort of Method 3, which is mainly due to the increasing number of fine-mesh DoFs in the patches. With increasing complexity of the multiscale problem, we thus expect even more speedups. We also note that the speedup w.r.t. the FOM method is also dependent on the outer iteration counts, cf. [39, 9]. It can be expected that the benefit of reduced models is even more present for increasing complexity of the optimization problem.

At the same time, as already mentioned before, in Table 4 the results confirm that our specific implementation leaves room for improvements concerning the construction of the Stage 2 model, which has an additional slow-down effect on the computational time.

| Evaluations | LOD | | St.1 | | St.2 | | $e^{\tilde{J}_h^{\text{loc}},\text{rel}}$ | | |
|-------------|-----|------|---------------|-----------|-----------------|-----------------|---|--------|----------|
| | FEM | Coa. | Local | Coa. | Local | O.it. | Time | | |
| Cost factor | h | H | $U(T_H)_h$ | H | N_{RB} | N_{RB} | | | |
| 3. PG-LOD | - | 307 | 665600 | - | - | - | 100 | 11317s | 2.07e-10 |
| 4. TR-TS | - | 10 | 32000 | 20 | 128000 | 938 | 5 | 5393s | 1.57e-10 |
| 4.r R-TR-TS | - | 8 | 51200 | 30 | 128000 | 422 | 4 | 2998s | 1.32e-11 |

Table 3: Experiment 2: Evaluations and accuracy of selected methods

| Method | Total | Speedup | Online | | Offline | | |
|-------------|--------|---------|--------|-------|---------|---------|---------|
| | | | outer | inner | FEM | Stage 1 | Stage 2 |
| 3. PG-LOD | 11317s | - | 11317s | - | - | - | - |
| 4. TR-TS | 5393s | 2 | 486s | 360s | - | 4042s | 505s |
| 4.r R-TR-TS | 2998s | 4 | 5s | 5s | - | 2690s | 336s |

Table 4: Experiment 2: More details on run times of selected methods

6 Concluding remarks and future work

In this article, we have combined localized reduced basis methods for efficiently solving parameterized multiscale problems with optimization methods that adaptively construct such localized reduced methods in the context of an iterative error-aware trust-region algorithm for accelerating PDE-constrained optimization. In particular, we have formulated a relaxed version of the TR-RB algorithm from [39] to neglect the strong certification in the first iterations. This relaxation has been advised so that the same convergence result holds asymptotically.

Subsequently, we have discretized the optimality system of the PDE-constrained optimization problem (P) with a localized ansatz based on the Petrov-Galerkin version of the localized orthogonal decomposition method. For an online efficient reduced model with optional local basis enrichment, such that the sub-problems of the TR algorithm can be solved fast, we have used the TSRBLOD based on a two-scale RB ansatz of the LOD.

The resulting TR-LRB method has proven advantageous both in terms of computational effort and adaptivity concerning the localized RB models. In the numerical experiments, we observed that these localized RB approaches can efficiently replace FEM-based techniques, especially for growing complexity of the multiscale system.

Many tasks have been left for the future. Although the underlying multiscale data is already highly heterogeneous and non-periodic, and the LOD approach showed good approximation properties w.r.t. FEM, it is commonly known that the LOD struggles, e.g., for high-contrast problems or complex coarse data such as thin channels. For using the TR-TSRBLOD, it has to be verified priorly that Assumption 3 is given up to an acceptable tolerance. To remedy this, the discussed concepts can be generalized to other multiscale methods, always dependent on the respective multiscale task. On the other hand, it would be desirable to derive a posteriori error theory for the LOD such that the homogenization term from (35) can be used to validate the approximation properties of the LOD, cf. Remark 4.8. Let us also mention that, in the work at hand, we have enforced several problem assumptions, e.g. ellipticity, symmetry, and homogeneous boundary conditions, to simplify the presentation of the algorithm. However, it is straightforward to generalize the methodology to more challenging problem classes.

Concerning the specific instance of the TR-TSRBLOD, the numerical experiments showed a significant overall speedup w.r.t. FEM and the PG-LOD with our implementation, and further improvements are possible. Our theoretical findings expect even better run times with an even more HPC-oriented implementational design. Moreover, an intermediate preparatory reduction of the two-scale system can be used to decrease further offline expenses of Stage 2.

Lastly, the described TR-LRB can be enhanced in terms of the choice of the local enrichment tolerance τ_{loc} , such that an appropriate choice for the respective optimization problem or model can efficiently be found with an adaptive refinements, cf. Section 4.4.

Code availability

All experiments have been implemented in Python using `gridlod` [26] for the PG-LOD discretization and `PyMOR` [45] for the model order reduction. In particular, the software is internally based on the software that has been used in [39] and [41]. The complete source code for all experiments, including setup instructions, can be found in [38].

References

- [1] Assyr Abdulle and Yun Bai. Reduced basis finite element heterogeneous multiscale method for high-order discretizations of elliptic homogenization problems. *Journal of Computational Physics*, 231(21):7014–7036, 2012.
- [2] Assyr Abdulle and Yun Bai. Adaptive reduced basis finite element heterogeneous multiscale method. *Computer Methods in Applied Mechanics and Engineering*, 257:203–220, 2013.

- [3] Assyr Abdulle and Yun Bai. Reduced-order modelling numerical homogenization. *Philosophical Transactions of the Royal Society A: Mathematical, Physical and Engineering Sciences*, 372(2021):20130388, 2014.
- [4] Assyr Abdulle, Yun Bai, and Gilles Vilmart. An offline–online homogenization strategy to solve quasilinear two-scale problems at the cost of one-scale problems. *International Journal for Numerical Methods in Engineering*, 99(7):469–486, 2014.
- [5] Assyr Abdulle and Andrea Di Blasio. Numerical homogenization and model order reduction for multiscale inverse problems. *Multiscale Modeling & Simulation*, 17(1):399–433, 2019.
- [6] Assyr Abdulle and Patrick Henning. A reduced basis localized orthogonal decomposition. *Journal of Computational Physics*, 295:379–401, 2015.
- [7] G. Allaire, C. Dapogny, A. Faure, and G. Michailidis. Shape optimization of a layer by layer mechanical constraint for additive manufacturing. working paper or preprint, November 2016.
- [8] Grégoire Allaire. *Shape optimization by the homogenization method*, volume 146. Springer Science & Business Media.
- [9] Stefan Banholzer, Tim Keil, Luca Mechelli, Mario Ohlberger, Felix Schindler, and Stefan Volkwein. An adaptive projected newton non-conforming dual approach for trust-region reduced basis approximation of pde-constrained parameter optimization. *arXiv preprint arXiv:2012.11653*, 2020.
- [10] M. Barrault, Y. Maday, N. C. Nguyen, and A. T. Patera. An ‘empirical interpolation’ method: application to efficient reduced-basis discretization of partial differential equations. *C. R. Math.*, 339(9):667–672, 2004.
- [11] Peter Benner, Albert Cohen, Mario Ohlberger, and Karen Willcox, editors. *Model reduction and approximation*, volume 15 of *Computational Science & Engineering*. Society for Industrial and Applied Mathematics (SIAM), Philadelphia, PA, 2017. Theory and algorithms.
- [12] S. Boyaval. Reduced-basis approach for homogenization beyond the periodic setting. *Multiscale Model. Simul.*, 7(1):466–494, 2008.
- [13] Donald L Brown and Daniel Peterseim. A multiscale method for porous microstructures. *Multiscale Modeling & Simulation*, 14(3):1123–1152, 2016.
- [14] Andreas Buhr, Laura Iapichino, Mario Ohlberger, Stephan Rave, Felix Schindler, and Kathrin Smetana. Localized model reduction for parameterized problems, 2021. In Benner, et.al.. *Model Order Reduction. Volume 2 Snapshot-Based Methods and Algorithms*. Walter De Gruyter GmbH, Berlin, 2021.
- [15] V. M. Calo, Y. Efendiev, J. Galvis, and M. Ghommem. Multiscale empirical interpolation for solving nonlinear PDEs. *J. Comput. Phys.*, 278:204–220, 2014.
- [16] S. Chaturantabut and D. C. Sorensen. Nonlinear model reduction via discrete empirical interpolation. *SIAM J. Sci. Comput.*, 32(5):2737–2764, 2010.
- [17] Rasmus E. Christiansen and Ole Sigmund. Designing meta material slabs exhibiting negative refraction using topology optimization. *Struct. Multidiscip. Optim.*, 54(3):469–482, 2016.
- [18] E. T. Chung, Y. Efendiev, and G. Li. An adaptive gmsfem for high-contrast flow problems. *J. Comput. Phys.*, 273:54–76, 2014.
- [19] Sergio Conti, Benedict Geihe, Martin Lenz, and Martin Rumpf. A posteriori modeling error estimates in the optimization of two-scale elastic composite materials. *ESAIM Math. Model. Numer. Anal.*, 52(4):1457–1476, 2018.
- [20] M. Drohmann, B. Haasdonk, and M. Ohlberger. Reduced basis approximation for nonlinear parametrized evolution equations based on empirical operator interpolation. *SIAM J. Sci. Comput.*, 34:A937–A969, 2012.
- [21] W. E and B. Engquist. The heterogeneous multi-scale method for homogenization problems. In *Multiscale methods in science and engineering*, volume 44 of *Lect. Notes Comput. Sci. Eng.*, pages 89–110. Springer, Berlin, 2005.
- [22] Y. Efendiev and T. Y. Hou. *Multiscale finite element methods: theory and applications*, volume 4. Springer Science & Business Media.
- [23] Yalchin Efendiev, Juan Galvis, and Thomas Y Hou. Generalized multiscale finite element methods (gmsfem). *Journal of computational physics*, 251:116–135, 2013.
- [24] Daniel Elfverson, Victor Ginting, and Patrick Henning. On multiscale methods in petrov–galerkin formulation. *Numerische Mathematik*, 131(4):643–682, 2015.

- [25] Subhendu Bikash Hazra and Volker Schulz. On efficient computation of the optimization problem arising in the inverse modeling of non-stationary multiphase multicomponent flow through porous media. *Comput. Optim. Appl.*, 31(1):69–85, 2005.
- [26] Fredrik Hellman and Tim Keil. gridlod. <https://github.com/fredrikhellman/gridlod>.
- [27] Fredrik Hellman, Tim Keil, and Axel Målqvist. Numerical upscaling of perturbed diffusion problems. *SIAM Journal on Scientific Computing*, 42(4):A2014–A2036, 2020.
- [28] Fredrik Hellman and Axel Målqvist. Contrast independent localization of multiscale problems. *Multiscale Modeling & Simulation*, 15(4):1325–1355, 2017.
- [29] Fredrik Hellman and Axel Målqvist. Numerical homogenization of elliptic pdes with similar coefficients. *Multiscale Modeling & Simulation*, 17(2):650–674, 2019.
- [30] P. Henning, A. Målqvist, and D. Peterseim. A localized orthogonal decomposition method for semi-linear elliptic problems. *ESAIM Math. Model. Numer. Anal.*, 48(5):1331–1349, 2014.
- [31] P. Henning, M. Ohlberger, and B. Schweizer. An adaptive multiscale finite element method. *Multiscale Model. Simul.*, 12(3):1078–1107, 2014.
- [32] Jan S. Hesthaven, Gianluigi Rozza, and Benjamin Stamm. *Certified reduced basis methods for parametrized partial differential equations*. SpringerBriefs in Mathematics. Springer, Cham; BCAM Basque Center for Applied Mathematics, Bilbao, Cham, 2016. BCAM SpringerBriefs.
- [33] Jan S. Hesthaven, Shun Zhang, and Xueyu Zhu. Reduced Basis Multiscale Finite Element Methods for Elliptic Problems. *Multiscale Modeling & Simulation*, 13(1):316–337, 2015.
- [34] Thomas Y Hou and Xiao-Hui Wu. A multiscale finite element method for elliptic problems in composite materials and porous media. *Journal of computational physics*, 134(1):169–189, 1997.
- [35] Thomas J.R. Hughes. Multiscale phenomena: Green’s functions, the dirichlet-to-neumann formulation, sub-grid scale models, bubbles and the origins of stabilized methods. *Computer Methods in Applied Mechanics and Engineering*, 127(1–4):387 – 401, 1995.
- [36] Thomas J.R. Hughes, Gonzalo R. Feijóo, Luca Mazzei, and Jean-Baptiste Quincy. The variational multiscale method—a paradigm for computational mechanics. *Computer Methods in Applied Mechanics and Engineering*, 166(1):3 – 24, 1998.
- [37] Jansen J.D. Adjoint-based optimization of multi-phase flow through porous media - a review. *Computers and Fluids*, 46(1):40 – 51, 2011. Cited by: 164.
- [38] Tim Keil. Software for: A relaxed localized trust-region reduced basis approach for optimization of multi-scale problems, 2022.
- [39] Tim Keil, Luca Mechelli, Mario Ohlberger, Felix Schindler, and Stefan Volkwein. A non-conforming dual approach for adaptive trust-region reduced basis approximation of pde-constrained parameter optimization. *ESAIM. Mathematical Modelling and Numerical Analysis*, 55(3):1239, 2021.
- [40] Tim Keil and Mario Ohlberger. Model reduction for large scale systems. *arXiv preprint arXiv:2105.01433*, 2021.
- [41] Tim Keil and Stephan Rave. An online efficient two-scale reduced basis approach for the localized orthogonal decomposition. *arXiv preprint arXiv:2111.08643*, 2021.
- [42] M. G. Larson and A. Målqvist. Adaptive variational multiscale methods based on a posteriori error estimation: duality techniques for elliptic problems. In *Multiscale methods in science and engineering*, volume 44 of *Lect. Notes Comput. Sci. Eng.*, pages 181–193. Springer, Berlin, 2005.
- [43] Axel Målqvist and Daniel Peterseim. Localization of elliptic multiscale problems. *Mathematics of Computation*, 83(290):2583–2603, 2014.
- [44] Axel Målqvist and Daniel Peterseim. *Numerical Homogenization by Localized Orthogonal Decomposition*. SIAM, 2020.
- [45] R. Milk, S. Rave, and F. Schindler. pyMOR, Model Order Reduction with Python, December 2014.
- [46] Axel Målqvist and Daniel Peterseim. Localization of elliptic multiscale problems. *Math. Comp.*, 83(290):2583–2603, Jun 2014.
- [47] N. C. Nguyen. A multiscale reduced-basis method for parametrized elliptic partial differential equations with multiple scales. *Journal of Computational Physics*, 227(23):9807–9822, 2008.

- [48] M. Ohlberger. A posteriori error estimates for the heterogeneous multiscale finite element method for elliptic homogenization problems. *Multiscale Model. Simul.*, 4(1):88–114, 2005.
- [49] M. Ohlberger and F. Schindler. A-posteriori error estimates for the localized reduced basis multi-scale method. In J. Fuhrmann, M. Ohlberger, and C. Rohde, editors, *Finite Volumes for Complex Applications VII-Methods and Theoretical Aspects*, volume 77 of *Springer Proceedings in Mathematics & Statistics*, pages 421–429. Springer International Publishing, 2014.
- [50] M. Ohlberger, B. Schweizer, M. Urban, and B. Verfurth. Mathematical analysis of transmission properties of electromagnetic meta-materials. *Networks and Heterogeneous Media*, 15(1):29–56, 2020.
- [51] Mario Ohlberger and Michael Schaefer. A reduced basis method for parameter optimization of multiscale problems. In *Proceedings of ALGORITMY*, volume 2012, pages 1–10, 2012.
- [52] Mario Ohlberger, Michael Schaefer, and Felix Schindler. Localized Model Reduction in PDE Constrained Optimization. In Volker Schulz and Diaraf Seck, editors, *Shape Optimization, Homogenization and Optimal Control : DFG-AIMS Workshop Held at the AIMS Center Senegal, March 13-16, 2017*, International Series of Numerical Mathematics, pages 143–163. Springer International Publishing, Cham, 2018.
- [53] Mario Ohlberger and Felix Schindler. Error control for the localized reduced basis multiscale method with adaptive on-line enrichment. *SIAM Journal on Scientific Computing*, 37(6):A2865–A2895, 2015.
- [54] Mario Ohlberger and Barbara Verfurth. A new heterogeneous multiscale method for the helmholtz equation with high contrast. *Multiscale Modeling & Simulation*, 16(1):385–411, 2018.
- [55] Daniel Peterseim and Robert Scheichl. Robust numerical upscaling of elliptic multiscale problems at high contrast. *Computational Methods in Applied Mathematics*, 16(4):579–603, 2016.
- [56] E. Qian, M. Grepl, K. Veroy, and K. Willcox. A certified trust region reduced basis approach to PDE-constrained optimization. *SIAM Journal on Scientific Computing*, 39(5):S434–S460, 2017.
- [57] A. Quarteroni, A. Manzoni, and F. Negri. *Reduced Basis Methods for Partial Differential Equations*, volume 92 of *La Matematica per il 3+2*. Springer International Publishing, Cham, 1 edition, 2016.
- [58] Fabian Wein, Nan Chen, Naveed Iqbal, Michael Stingl, and Marc Avila. Topology optimization of unsaturated flows in multi-material porous media: application to a simple diaper model. *Commun. Nonlinear Sci. Numer. Simul.*, 78:104871, 16, 2019.
- [59] E. Weinan, Björn Engquist, and Zhongyi Huang. Heterogeneous multiscale method: a general methodology for multiscale modeling. *Physical Review B*, 67(9):092101, 2003.
- [60] Yao. Yue and Karl. Meerbergen. Accelerating optimization of parametric linear systems by model order reduction. *SIAM Journal on Optimization*, 23(2):1344–1370, 2013.